*Revue Roumaine de Chimie*, **2007**, *52*(8–9), 829–835

*Dedicated to Professor Victor-Emanuel Sahini on the occasion of his 80th anniversary*

# QSAR ANALYSIS OF A SERIES OF NON-IMIDAZOLIC DERIVATIVES ACTING ON THE HISTAMINE H3 RECEPTOR

Maria MRACEC,* Ana BOROTA, Ramona RAD, Liliana OSTOPOVICI and Mircea MRACEC

Roumanian Academy Institute of Chemistry Timisoara, Bd. Mihai Viteazul Nr. 24, RO-300223 Timisoara, Roumania, e-mail: mmracec@acad-icht.tm.edu.ro

*Received December 28, 2006*

A QSAR study using multiple linear regression (MLR) is reported for a series of non-imidazolic antagonists of the histamine H3 receptor. One of the best models contains four descriptors: $DM_H$ (sp hybridization component of the AM1 dipole moment), HYE (hydration energy), logP and S_110 (number of –SO2- groups) and has statistical indices: n = 30 $r^2$ = 0.955 $r^2_{adj}$ = 0.948 $r^2_{CV(LOO)}$ = 0.925 see = 0.215 F = 132.32 press = 1.155. The antihistaminic activity of the ligands is influenced by their electronic, hydrophobicity and thermodynamic properties.

## INTRODUCTION

Histamine is an endogenous amine that acts as neurotransmitter. It is implicated in gastric secretion of HCl and pepsin, in bronchoconstriction, in pain and prurit. It produces different effects in the circulatory and the central nervous systems. Physiological effects of histamine are due to the activation of four receptor subtypes, namely H1 – H4. The H3 subtypes act both as presynaptic autoreceptors[1] and postsynaptic receptors[2] in central nervous system (CNS). The H3 antagonists have potential therapeutic applications in different CNS diseases: epilepsia, schizophrenia, insomnia, sleeping disease, bullimia, Alzheimer's disease, temporary loss of memory and incapacity of learning.[3-10] The search for novel histamine H3 receptor ligands with drug-like properties has resulted in the discovery of an increasing number of imidazole-free structures with improved pharmacokinetic and pharmacodynamic properties. We report here the results of a classical quantitative structure-activity relationships (QSARs) study for a series of non-imidazolic compounds synthesized and tested by Hancock et all[11] as antagonists on the guinea pig brain H3 receptor.

## METHODS

The structure and activities obtained by Hancock et all[11] for a series of 31 pyrrolidinic derivatives, together with a series of 14 derivatives of 2,5-diazabiciclo[2.2.1]heptane are displayed in Table 1. Antihistaminic activity has been expressed as the negative logarithm of inhibition constant (molarity units), pKi.

Molecular geometries of derivatives from both series have been optimized using the AMBER99 force field and then the AM1 Hamiltonian.[12] Optimization was performed with Polak- Ribiere conjugate gradient algorithm, method which is implemented in HyperChem7.52.[13] The geometry was optimized till the RMS gradient was equal to or less than 0.01 kcal/Åmol. For some representative structures a conformational search has been carried out[14,15] with the Conformational Search module also available in Hyperchem7.52.

Lowest AM1 energies are obtained for conformers with two neighbor carbonylic groups in *anti* positions. Similarly, the lowest energy was obtained for conformers with the H and carbonyl in the amidic group in *anti* positions. For example, for compound **5,** the most stable conformer with *anti* positions both for carbonylic groups and

amidic hydrogens the $\Delta H_f$ is -213.755 kcal/mol. A conformer with the amidic H and carbonylic group in *syn* position has a formation energy of -210.656 kcal/mol. The conformer of compound **5** with the lowest energy is presented in Fig 1. The possibility of stabilization of conformers by intramolecular H bonds was checked. Such stabilization could not be evidenced neither for the conformers obtained with the AMBER99 force field nor for those obtained with the AM1 Hamiltonian.

For calculating the descriptors to be tested in multiple linear regressions, the QSAR properties module from the HyperChem7.52 and DRAGON3.0[16] sofwares have been used. From the AM1 method the energies of the highest occupied molecular orbital, $E_{HOMO}$ and of the lowest unoccupied molecular orbital $E_{LUMO}$, the total dipole moment and the *sp* hybridization component of the dipole moment have been obtained. The absolute electronegativity ($\chi$) and the chemical hardness ($\eta$) have been calculated as $\chi \approx (IP+ EA)/2$ and $\eta \approx (IP - EA)/2$ assuming that the ionization potential, $IP \approx - E_{HOMO}$ and the electron affinity, $EA \approx - E_{LUMO}$.[17,18] From the AM1 method resulted also a thermodynamic property, namely, the energy of formation, $\Delta H_f$. As descriptors have also been tested the energy terms (bond, angle, torsion and van der Waals energies) resulted for geometries of conformers optimized with the AMBER99 force field.

*Table 1*
The structure and antihistaminic activity of pyrrolidinic and 2,5-diazabiciclo[2.2.1]heptane derivatives

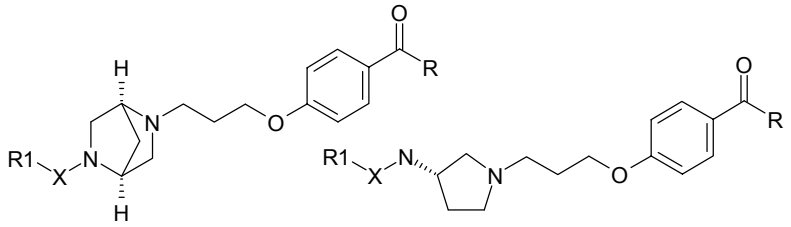


structure B structure A

| No. | Struct | R | X | $R_1$ | pKi |
|---|---|---|---|---|---|
| 5 | A | $CH_3$ | -CO- | Boc L-Ala | 6.05 |
| 6 | A | $CH_3$ | -CO- | Boc D-Ala | 6.51 |
| 7 | A | $CH_3$ | -CO- | Boc L-Ser | 6.23 |
| 8 | A | $CH_3$ | -CO- | Boc D-Ser | 6.51 |
| 9 | A | $CH_3$ | -CO- | L-Ser | 6.82 |
| 10 | A | $CH_3$ | - | - | 5.76 |
| 11 | A | $CH_3$ | - | - | 6.17 |
| 12 | A | $CH_3$ | -CO- | 2-pyrazinyl | 6.69 |
| 13 | A | $CH_3$ | -CO- | 3-pyridyl | 7.43 |
| 14 | A | $CH_3$ | -CO- | 4-thiazol[2-(3-pyridyl)]yl | 7.26 |
| 15 | A | $CH_3$ | -CO- | p-CN-phenyl | 7.4 |
| 16 | A | Cyclopropyl | -CO- | 4-thiazol[2-(3-pyridyl)]yl | 7.3 |
| 31 | A | $CH_3$ | $-SO_2-$ | p-CN phenyl | 8.22 |
| 32 | A | Cyclopropyl | $-SO_2-$ | p-CN phenyl | 8.4 |
| 33 | A | Cyclopropyl | $-SO_2-$ | Phenyl | 8.52 |
| 34 | A | Cyclopropyl | $-SO_2-$ | o-F phenyl | 8.57 |
| 35 | A | Cyclopropyl | $-SO_2-$ | m-F phenyl | 8.8 |
| 36 | A | Cyclopropyl | $-SO_2-$ | p-F phenyl | 8.46 |
| 37 | A | Cyclopropyl | $-SO_2-$ | o-Cl phenyl | 8.43 |
| 38 | A | Cyclopropyl | $-SO_2-$ | m-Cl phenyl | 8.52 |
| 39 | A | Cyclopropyl | $-SO_2-$ | p-Cl phenyl | 8.42 |
| 40 | A | Cyclopropyl | $-SO_2-$ | o-CN phenyl | 7.96 |
| 41 | A | Cyclopropyl | $-SO_2-$ | m-CN phenyl | 8.55 |
| 42 | A | Cyclopropyl | $-SO_2-$ | o-$CH_3$ phenyl | 7.96 |
| 43 | A | Cyclopropyl | $-SO_2-$ | m-$CH_3$ phenyl | 8.57 |
| 44 | A | Cyclopropyl | $-SO_2-$ | p-$CH_3$ phenyl | 8.38 |
| 45 | A | Cyclopropyl | $-SO_2-$ | p-$OCH_3$ phenyl | 8.54 |
| 46 | A | Cyclopropyl | $-SO_2-$ | 4 (t-butyl)phenyl | 8.28 |
| 47 | A | Cyclopropyl | $-SO_2-$ | p-Br phenyl | 8.3 |
| 48 | A | Cyclopropyl | $-SO_2-$ | 4-(ethyl) phenyl | 8.34 |
| 49 | A | Cyclopropyl | $-SO_2-$ | N-$CH_3$-imidazol-4-yl | 8 |
| 17 | B | Cyclopropyl | -CO- | Boc D-Ala | 6.51 |
| 18 | B | Cyclopropyl | -CO- | Boc L-Ala | 5.66 |
| 19 | B | Cyclopropyl | -CO- | D-Ala | 6.38 |

*Tab. 1. (continued)*

| | structure B | | structure A | | |
|---|---|---|---|---|---|
| No. | Struct | R | X | $R_1$ | pKi |
| 20 | B | Cyclopropyl | -CO- | L-Ala | 6.63 |
| 21 | B | Cyclopropyl | -CO- | cyclohexyl | 6.87 |
| 22 | B | Cyclopropyl | -CO- | Phenyl | 6.46 |
| 23 | B | Cyclopropyl | -CO- | p-F phenyl | 6.59 |
| 24 | B | Cyclopropyl | -CO- | 2-pyridyl | 6.72 |
| 25 | B | Cyclopropyl | -CO- | 2-furyl | 6.68 |
| 26 | B | Cyclopropyl | -CO- | $CH_2C(CH_3)_3$ | 5 |
| 27 | B | Cyclopropyl | -CO- | Boc β-Ala | 7.15 |
| 28 | B | Cyclopropyl | -CO- | β-Ala | 7.77 |
| 50 | B | Cyclopropyl | $-SO_2-$ | Ethyl | 6.92 |
| 51 | B | Cyclopropyl | $-SO_2-$ | Phenyl | 7.72 |

Statistical data were obtained with STATISTICA 5.0. The descriptor elimination was carried out using the forward stepwise regression method included in STATISTICA 5.0. Outliers are considered compounds for which the pKi calculated values are outside of the interval of ±2 sigma.

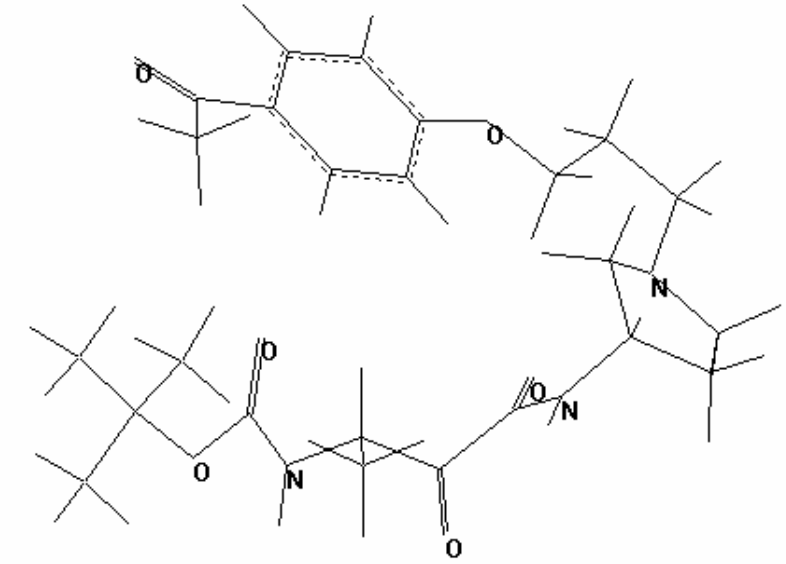


Fig 1 – The structure of the best conformer (with the lowest energy) of compound **5** resulted from AM1 calculations; the two vicinal carbonyl groups in *anti* positions together with the hydrogen atom and the cabonylic oxygen of the amidic group.

## RESULTS

Statistical parameters of some monolinear regressions after the elimination of outliers are presented in Table 2. From this table one can see that some structures (27, 28, 18, 22) are eliminated in many regressions and structure 26 is outlier in almost all regressions.

*Table 2*

Statistical values of monoparametric regressions after elimination of outliers

| Descriptors | **r** | **s** | **F** | **n** | **Outliers** |
|---|---|---|---|---|---|
| $E_{BOND}$ (kcal/mol) | 0.977 | 0.190 | 535.54 | 28 | 5,7,8,9,10,11,13,17,19,20,25,26,27,28,46,49,50 |
| $DM_H$ (debye) | 0.963 | 0.233 | 349.34 | 29 | 5,8,10,11,13,14,18,19,20,24,26,28,31,32,47,50 |
| MOR26M | 0.971 | 0.194 | 461.03 | 30 | 5,6,7,8,9,10,18,19,22,26,28,33,35,39,49 |
| NS | 0.974 | 0.215 | 580.71 | 33 | 5,10,13,14,15,16,18,26,27,28,50,51 |
| S_110 | 0.974 | 0.215 | 580.71 | 33 | 5,10,13,14,15,16,18,26,27,28,50,51 |

*Tab. 1. (continued)*

| | | | | | |
|---|---|---|---|---|---|
| MOR26V | 0.928 | 0.315 | 193.70 | 33 | 5,6,7,8,10,12,15,18,22,26,28,49 |
| MOR11U | 0.967 | 0.248 | 456.38 | 34 | 6,11,12,21,22,23,26,27,28,43,46 |
| R2E | 0.953 | 0.267 | 316.36 | 34 | 5,10,11,15,18,19,26,27,46,49,51 |
| MOR20M | 0.952 | 0.321 | 312.92 | 34 | 10,11,12,13,15,21,22,23,27,28,47* |
| R1M_ | 0.947 | 0.279 | 303.68 | 37 | 5,10,11,18,26,27,28,47 |
| HOMT | 0.807 | 0.594 | 80.43 | 37 | 14,16,22,23,26,27,28,49 |
| MOR11P | 0.948 | 0.296 | 319.57 | 38 | 7,10,12,17,26,27,28 |
| MOR11E | 0.947 | 0.316 | 314.94 | 38 | 12,21,23,26,27,28,46 |
| MAXDN | 0.898 | 0.380 | 149.43 | 38 | 5,7,10,18,26,28,50 |
| N_072 | 0.939 | 0.331 | 276.68 | 39 | 12,19,22,26,27,50 |
| MOR06M | 0.908 | 0.390 | 172.78 | 39 | 5,13,18,26,28,50 |
| MOR11M | 0.943 | 0.323 | 306.65 | 40 | 12,17,26,27,28 |
| HATS1M | 0.888 | 0.430 | 141.92 | 40 | 10,26,28,46,47 |
| MOR26P | 0.887 | 0.430 | 139.96 | 40 | 7,10,26,28,49 |
| R1M | 0.914 | 0.378 | 196.91 | 41 | 18,26,28,47 |
| BEHP1 | 0.900 | 0.409 | 166.11 | 41 | 13,18,26,51 |
| logP | 0.736 | 0.618 | 46.02 | 41 | 18,22,23,26 |
| HYE (kcal/mol) | 0.737 | 0.683 | 47.63 | 42 | 7,8,9* |
| RDF040M | 0.862 | 0.485 | 118.67 | 43 | 26,28 |
| $E_{BEND}$ (kcal/mol) | 0.564 | 0.756 | 19.16 | 43 | 18,26 |
| E (kcal/mol) | 0.563 | 0.757 | 19.04 | 43 | 18,26, |
| MW | 0.394 | 0.842 | 7.53 | 43 | 18,26, |
| DM (debye) | 0.693 | 0.682 | 38.90 | 44 | 26 |
| $E_{HOMO}$ (eV) | 0.627 | 0.738 | 27.21 | 44 | 26 |
| $E_{LUMO}$ (eV) | 0.627 | 0.738 | 27.15 | 44 | 26 |
| NMB | 0.666 | 0.750 | 34.19 | 45 | - |
| X (eV) | 0.637 | 0.775 | 29.40 | 45 | - |

**r** – correlation coefficient; **see** – standard error of estimate; **F** – F ratio; **n** – number of cases; **E** – potential energy of a conformer calculated with the AMBER99 method; $E_{BOND}$ and $E_{BEND}$ – stretching and bending energy terms calculated with AMBER99 force field; $E_{HOMO}$ and $E_{LUMO}$ – AM1 energies of the highest occupied and of the lowest unoccupied molecular orbitals; DM – AM1 total dipole moment; $DM_H$ – sp hybridization component of AM1 dipole moment; HyE – hydration energy; absolute electronegativity, $\chi = ½ (IP+EA)$; chemical hardness, $\eta = ½ (IP-EA)$; log P – log of the n-octanol-water partition coefficient; MW – molecular weight; NMB – number of multiple bonds; NS – number of sulfur atoms; MAXDN –maximal electropological negative variation; BEHP1 – highest eigenvalue n.1 of Burden matrix/weighted by atomic polarizabilities; HOMT – total HOMA (harmonic oscillator model of aromaticity index); RDF040M – radial distribution function – 4.0/weighted by atomic masses; Mor11u – 3D-MoRSE - signal 11 unweighted; Mor06m – 3D-MoRSE - signal 06/weighted by atomic masses; Mor11m – 3D-MoRSE - signal 11/weighted by atomic masses; Mor20m – 3D-MoRSE - signal 20/weighted by atomic masses; Mor26m – 3D-MoRSE - signal 26/weighted by atomic masses; Mor11v – 3D-MoRSE - signal 11/weighted by atomic van der Waals volumes; Mor26v – 3D-MoRSE - signal 26/weighted by atomic van der Waals volumes; Mor11e – 3D-MoRSE - signal 11/weighted by atomic Sanderson electronegativities; Mor11p – 3D-MoRSE - signal 11/weighted by atomic polarizabilities; ; Mor26p – 3D-MoRSE - signal 26/weighted by atomic polarizabilities; R1m – R autocorrelation of lag 1/weighted by atomic masses; R1m_ – R maximal autocorrelation of lag1/weighted by atomic masses; R2e – R autocorrelation of lag 2/weighted by atomic Sanderson electronegativities; N_072 – number of RCO-N< / >N-X=X groups; S110 – number of R-SO2-R groups.

Some descriptors can model by themselves the pKi values (Table 2). However, associating the descriptors with physical meaning the resulted multiple linear regressions have better chances to model the histaminic activity.

The regression (1) results by associating the $E_{BOND}$, DM, $DM_H$, SASA, HYE after elimination of outliers 7, 18, 21, 28:

$$pKi = 2.4375(0.6793) - 06410(0.1906)E_{BOND} + 0.3068(0.0403)\ DM + +0.4925(0.1470)DM_H + 0.0039(0.0008)SASA - 0.1216(0.0274)HYE \quad (1)$$

$$n = 41 \quad r^2 = 0.899 \quad r^2_{adj} = 0.885 \quad see = 0.333 \quad F = 62.40 \quad press = 3.89$$

This model suggests that the interactions of the derivatives with the histamine H3 receptor could be significantly influenced by: thermodynamic stability of conformers (HYE), electrostatic effects (DM), solvent effects (SASA, HYE) and possibility of H bond formation ($DM_H$). The cross-correlation matrix in Table 3 shows that there is no significant statistical cross-correlation between the descriptors of the regression (1).

*Table 3*

Values of partial and cross-correlation coefficients for regresstion (1)

| | $E_{BOND}$ | DM | $DM_H$ | SASA | HYE |
|---|---|---|---|---|---|
| DM | -0.223 | | | | |
| $DM_H$ | -0.496 | 0.426 | | | |
| SASA | 0.067 | 0.072 | 0.138 | | |
| HYE | 0.624 | -0.060 | -0.353 | -0.098 | |
| pKi | -0.651 | 0.649 | 0.696 | 0.336 | -0.607 |

If in regression (1) instead of SASA is used as descriptor log P, results regression (2). After elimination of outliers 18, 26, 28, regression (2) is:

$$pKi = 5.0731(0.3773) - 0.4474(0.1550)\, E_{BOND} + 0.1645(0.0378)DM + \\ +0.4724(0.1217)\, DM_H - 0.1222(0.0220)\, HYE + 0.3764(0.0503)\log P \quad (2)$$
$$n = 42 \quad r^2 = 0.918 \quad r^2_{adj} = 0.907 \quad see = 0.279 \quad F = 80.87 \quad press = 2.81$$

The cross-correlation matrix for regression (2) is displayed in Table 4. Cross-correlation coefficients and other statistical parameters (r, see, F) are better than those in equation (1). log P in equation (2) suggests that for these two series of compounds the transmembranar transport (high hydrophobicity) is important for the antihistaminic activity.

*Table 4*

Values of partial and cross-correlation coefficients for regresstion (2)

| | $E_{BOND}$ | DM | $DM_H$ | HYE | log P |
|---|---|---|---|---|---|
| DM | -0.252 | | | | |
| $DM_H$ | -0.444 | 0.447 | | | |
| HYE | 0.580 | -0.111 | -0.234 | | |
| log P | -0.149 | 0.556 | 0.379 | 0.045 | |
| pKi | -0.609 | 0.695 | 0.672 | -0.500 | 0.689 |

To validate equation (2), the compounds have been divided into two series. Test series contained compounds: 6,8,14,19,32,36,37,38. The regression for the learning series is:

$$pKi = 4.9973(0.429) - 0.4523(0.186)\, E_{BOND} + 0.1892(0.050)DM + 0.5062(0.175)DM_H - 0.1128(0.026)HYE + \\ 0.3543(0.061)\log P \quad (3)$$
$$n = 34 \quad r^2 = 0.906 \quad r^2_{adj} = 0.890 \quad see = 0.303 \quad F = 54.18 \quad press = 2.57$$

The cross-correlation matrix corresponding to regression (3) is displayed in Table 5 and the pKi values of the test compounds predicted by regression (3) are presented in Table 6. The calculated activities are shifted to weaker potency than the experimental one and differ with more than 0.5 log units.

By associating the $DM_H$, HYE, logP and S_110 descriptors, another statistical significant regression was obtained. After eliminating the outliers 5,18,19,25-28,40, regression (4) resulted:

$$pKi = 4.8352(0.1738) + 0.7305\,(0.1037)DM_H - 0.1358\,(0.0171)HYE + 0.3748(0.0441)\log P + \\ +0.4347\,(0.1229)S\_110 \quad (4)$$
$$n = 37 \quad r^2 = 0.957 \quad r^2_{adj} = 0.951 \quad see = 0.201 \quad F = 176.82 \quad press = 1.292$$

*Table 5*

Values of partial and cross-correlation coefficients for regresstion (3)

| | $E_{BOND}$ | DM | $DM_H$ | HYE | log P |
|---|---|---|---|---|---|
| $E_{BOND}$ | 1.000 | | | | |
| DM | -0.177 | 1.000 | | | |
| $DM_H$ | -0.478 | 0.529 | 1.000 | | |
| HYE | 0.587 | -0.168 | -0.281 | 1.000 | |
| log P | -0.004 | 0.515 | 0.441 | 0.119 | 1.000 |
| pKi | -0.542 | 0.711 | 0.751 | -0.492 | 0.636 |

*Table 6*

Experimental and predicted pKi values
by regression (3) for the test set compounds

| no | $pKi_{exp}$ | $pKi_{pred}$ | diff |
|---|---|---|---|
| 6 | 6.513 | 6.387 | 0.126 |
| 8 | 6.509 | 6.041 | 0.468 |
| 14 | 7.260 | 7.364 | -0.105 |
| 19 | 6.384 | 6.553 | -0.169 |
| 32 | 8.398 | 8.325 | 0.073 |
| 36 | 8.456 | 8.397 | 0.059 |
| 37 | 8.432 | 8.265 | 0.167 |
| 38 | 8.523 | 8.516 | 0.007 |

Diff – difference: pKi(exp ) – pKi(pred)

Regresion (4) suggests that the number of the -SO2- groups influence favorably the antihistaminic potency; the greater the number of –SO2- groups, the higher the activity. Cross-correlation and partial correlation coefficients are displayed in Table 7.

*Table 7*

Values of partial and cross-correlation coefficients for equation (4)

| | $DM_H$ | HYE | logP | S_110 |
|---|---|---|---|---|
| HYE | -0.367 | | | |
| logP | 0.419 | 0.143 | | |
| S_110 | 0.814 | -0.411 | 0.563 | |
| pKi | 0.841 | -0.519 | 0.648 | 0.889 |

The predictive potential of the regression was verified by the usual procedure. The 37 compounds have been divided into learning and test sets. By eliminating the test set compounds: 7,12,14,31,42,43,51, the regression (5) was obtained.

$$pKi = 4.8030(0.2085) + 0.8092(0.1638)\ DM_H - 0.1354(0.0197)\ HYE + 0.3694(0.0499)logP + 0.3627(0.1644)S\_110 \quad (5)$$

$$n = 30\ \ r^2 = 0.955\ \ r^2_{adj} = 0.948\ \ r^2_{CV(LOO)} = 0.925\ \ s = 0.215\ \ F = 132.32\ \ press = 1.155$$

pKi values calculated with equation (5) are shown in Table 8. Although two descriptors strongly cross-correlate the predicted pKi values are unexpectedly good.

*Table 8*

pKi values calculated with regression (5) for test series

| no | $DM_H$ | HYE | logP | S_110 | $pKi_{exp}$ | $pKi_{pred}$ | Diff |
|---|---|---|---|---|---|---|---|
| 7 | 0.332 | -7.71 | 0.72 | 0 | 6.231 | 6.381 | -0.150 |
| 12 | 0.609 | -6.29 | 1.20 | 0 | 6.695 | 6.590 | 0.104 |
| 14 | 1.999 | -5.45 | 1.04 | 0 | 7.260 | 7.542 | -0.283 |
| 31 | 0.874 | -10.85 | 2.08 | 1 | 8.222 | 8.110 | 0.112 |
| 42 | 1.508 | -6.12 | 1.80 | 1 | 7.959 | 7.879 | 0.080 |
| 43 | 1.535 | -6 | 3.20 | 1 | 8.569 | 8.402 | 0.167 |
| 51 | 1.244 | -5.3 | 2.54 | 1 | 7.721 | 7.828 | -0.107 |

## CONCLUSIONS

Antihistaminic activity of substituted pyrrolidinic derivatives can be modeled by many descriptors. pKi is influenced by electronic, hydrophobicity, steric and thermodynamic descriptors. The majority of models are based on stretching energy and SASA descriptors. Models with predictive potential give some suggestions regarding the influence of different properties on the antihistaminic activity. Stretching energies, hydration energies and number of peptidic bonds are inverse proportionally related to the antihistaminic potency and the rest of descriptors used in predictive models are directly proportional related to pKi. Models obtained suggest that antihistaminic activity is influenced by conformational stability of ligands, their degree of unsaturation, their electrostatic properties and hydrophobicity.

## REFERENCES


1. J.-M. Arrang, M. Garbarg and J.-C. Schwartz, *Nature (London)*, **1983**, *302*, 832-837.
2. E. Schlicker, R. Betz and M. Göthert, *Arch. Pharmacol*., **1988**, *337*, 588-590.
3. M. Passani, J.S. Lin, A.A. Hancock, S.P. Crochet and P. Blandina, *Trends Pharmacol Sci*., **2004**, *25*, 618-25.
4. P.L. Chazot and V. Hann, *Curr. Opin. Invest. Drugs,* **2001**, *2*, 1428-1431.
5. R. Leurs, R.A. Bakker, H. Timmerman and I.J. de Esch, *Nat. Rev. Drug Discov*., **2005**, *4*, 107-20.
6. M. Cowart, R. Altenbach, L. Black, R. Faghih, C. Zhao and A.A. Hancock, *Mini-Reviews in Medicinal Chemistry*, **2004**, *9*, 979-92.
7. B.B. Yao, C.W. Hutchins, T.L.Carr, S. Cassar, J.N. Masters, Y.L. Bennani, T.A. Esbenshade and A.A. Hancock, *Neuropharmacology*, **2003**, *44*, 773-86.
8. G.B. Fox, T.A. Esbenshade, J.B. Pan, R.J. Radek, K.M. Krueger, B.B. Yao, K.E. Browman, M.J. Buckley, M.E. Ballard, V.A. Komater, H. Miner, M. Zhang, R. Faghih, L.E. Rueter, R.S. Bitner, K.U. Drescher, J. Wetter, K. Marsh, M. Lemaire, R.D. Porsolt, Y.L. Bennani, J.P. Sullivan, M.D. Cowart, M.W. Decker and A.A.Hancock, *J. Pharmacol. Exp. Ther*., **2005**, *313*, 176-90.
9. J.M. Witkin and D.L. Nelson, *Pharmacol Ther*., **2004**, *103*, 1-20.
10. M. Zhang, M.E. Ballard, L. Pan, S. Roberts, R. Faghih, M. Cowart, T.A. Esbenshade, G.B. Fox, M.W. Decker, A.A. Hancock and L.E. Rueter, *Brain Res*., **2005**, *1045*, 142-9.
11. A.Vasudevan, S.E. Conner, R.G. Gentles, R. Faghih, H. Liu, W. Dwight, L. Ireland, C.H. Kang, T.A. Esbenshade, Y.L. Bennani and A.A. Hancock *Bioorg. Med. Chem. Lett.,* **2002**, *12*, 3055
12. M.J.S Dewar, E.G. Zoebisch, E.F. Healy and J.J.P. Stewart, *J. Am. Chem. Soc.*, **1985**, 107, 3902-3909.
13. HyperChem$^{(R)}$ release 7,52 for Windows, Hypercube, Inc. 2006.
14. A. Borota, M. Mracec, R. Rad, L. Ostopovici and M. Mracec, *Int. J. Quant. Chem.,* **2007**, *107*, 1803-1813.
15. M. Mracec, A. Borota, R. Rad, L. Ostopovici and M. Mracec, *Rev Roum. Chim.,* **2007**, *52*, 201-206.
16. R. Todeschini, V. Consonni, A. Mauri and M. Pavan, DRAGON 3.0, **2003**.
17. R.G. Parr and R.G. Pearson, *J. Am. Chem. Soc.,* **1983**, *105*, 7512-7516.
18. R.G. Pearson, *Chemtracts-Inorg. Chem.,* **1991**, *3*, 317-333.

*Revue Roumaine de Chimie*, **2007**, *52*(8–9), 837–844

*Dedicated to Professor Victor-Emanuel Sahini on the occasion of his 80th anniversary*

# CONFORMATIONAL ANALYSIS WITH AMBER AND AM1 METHODS OF A PARTIAL AGONIST, (R)-2-[(4-PHENYL-BUTYLAMINO)-METHYL]-CHROMAN-7-OL ACTIVE ON THE DOPAMINIC D2 RECEPTOR

Liliana OSTOPOVICI, Ramona RAD, Ana BOROTA, Maria MRACEC* and Mircea MRACEC

Roumanian Academy, Institute of Chemisty, Timisoara, 24 M.Viteazu Av., 300223-Roumania
e-mail: mmracec@acad-icht.tm.edu.ro

*Received May 29, 2007*

2-[(4-Phenyl-butylamino)-methyl]-chroman-7-ol, a high active partial agonist acting on the dopamine D2 receptor was chosen for a conformational analysis using the AMBER99 force field and the AM1 semiempirical quantum-chemical methods. The geometric properties of its conformers that occupy the low minima on the potential energy surface have been evaluated. Of 100 conformers retained from conformational search by optimization with AMBER force field had resulted only 38 distinct conformers which were distributed on an energy domain of 1.72kcal/mol above the lowest energy conformer. The conformers occupy a large space around the chromane moiety, but according to rotation barriers the ligand can modify its conformation to one suitable for efficient interaction with the amino acid residues from the active site of the D2 receptor.

## INTRODUCTION

Molecular cloning techniques have led to the characterization of a number of dopamine receptor subtypes which can be divided into the D1-like and the D2-like families. Whereas the D1-like family comprises D1 and D5 subtypes the D2-like family consists of D2, D3 and D4 receptors. According to neuropathological and genetic studies, selective dopamine D2 and D4 receptor agonists, partial agonists or antagonists might be of interest for the treatment of neuropsychiatric disorders including attention deficit hyperactivity, mood disorders and Parkinson's disease.[1-3]

On the other hand, the D3 receptor appears an important target for the development of candidate drugs since it is selectively expressed in the brain limbic system, which is thought to be involved in mood and cognitive disturbances as well as drug dependence. Thus, studies with respect to D2, D3 and D4 affinity, selectivity and ligand efficacy are of special current interest, as well as studies regarding ligand properties responsible for the biological activity.

Among synthesized ligands we choose to study the influence of steric factors onto biological activity of the 2-[(4-phenyl-butylamino)-methyl]-chroman-7-ol ligand having $K_{i\text{-}high}$ and $K_{i\text{-}low}$ values determined for both the high- and low-affinity agonist states of the dopamine D2 receptor ($D_2^{high}$ and $D_2^{low}$).[4] In this study we use two different molecular modelling methods for obtaining the geometry of conformers occupying the low minima on potential energy surface of this high potent partial agonist. The data can help in emphasizing the importance of steric effects, hydrogen bonds and van der Waals interactions of conformers with different residues from the active site of the D2 receptor.

## METHODS

For the purpose of modelling of the ligand geometry we use one molecular mechanics method, namely the AMBER99 force field, and a semiempirical quantum chemical method, AM1.[5]

The starting 2D-geometry of the 2-[(4-phenyl-butylamino)-methyl]-chroman-7-ol ligand was transformed into a 3D-geometry using the Model Builder module from Hyperchem7.52 package.[6]

The conformational analysis was performed with the Conformational search module from Hyper7.52 using the AMBER99 force field. This ligand has 7 rotatable bonds. Therefore seven dihedrals: $O_1$-$C_2$-$C_{11}$-$C_{12}$ (D1), D2 $C_2$-$C_{11}$-$N_{12}$-$C_{13}$ (D2), $C_{11}$-$N_{12}$-$C_{13}$-$C_{14}$ (D3), $N_{12}$-$C_{13}$-$C_{14}$-$C_{15}$ (D4), $C_{13}$-$C_{14}$-$C_{15}$-$C_{16}$ (D5), $C_{14}$-$C_{15}$-$C_{16}$-$C_{17}$ (D6) and $C_{15}$-$C_{16}$-$C_{17}$-$C_{18}$ (D7) have been varied between 0° and 360° with steps of 60°. The structure of the ligand and the numbering of heavy atoms is depicted in Fig 1.

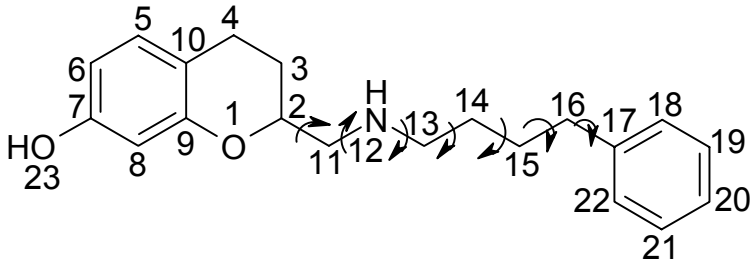


Fig. 1 – Numbering of atoms in (R)-2-[(4-phenyl-butylamino)-methyl]-chroman-7-ol and the dihedrals varied in conformational analysis.

In order to choose the starting conformations the conformer analysis was performed with Usage Direct method. The acceptance energy criterion was set at 100 kcal/mol above the energy of the best conformer. Standard preoptimization tests were carried out and the conformers that changed their chirality have been discarded. Two optimization criteria have been used: the maximum number of optimization cycles was set to 5000 and the RMS gradient norm was set to 0.01 kcal/Åmol. Search stop was achieved when the number of optimized conformers was 5000.

The 100 lowest energy conformations resultated from conformational search were further completely optimized with the AM1 semiempirical MO method as implemented in HyperChem7.52. The criteria set in AM1 optimization were: a RMS gradient norm of 0.01kcal/Åmol and a SCF convergence of $10^{-5}$. Optimization was performed with the algorithm Polak-Ribiere conjugate gradient.

## RESULTS AND DISCUSSION

Of 100 conformers given by conformational search with AMBER force field only 38 distinct conformers resulted. Their energy and dihedral values are presented in Table 1.

The distribution of conformers is not uniform. In the thermal energy domain (namely 0-0.6 kcal/mol) there are only two conformers with potential energy above the energy of the best conformer. In the energy domain 0.5 -1 kcal/mol there are four conformers, in the energy domain 1-1.5kcal/mol there are 19 conformers and in the energy domain 1.5 – 1.72 kcal/mol there are 12 conformers.

The superposition of the conformers in the energy domain 0 – 1 kcal/mol is presented in Fig. 2, while the superposition of the conformers in the energy domain 0 – 1.5kcal/mol is presented in Fig. 3.

Analyzing Figs 2 and 3 one can see that the space occupied by the side chain bound at 2-position of the chromane moiety is very large.

*Table 1*

Energy and dihedral values for 100 lowest energy conformers resulted from conformational search with AMBER99 method

| No | E | D1 | D2 | D3 | D4 | D5 | D6 | D7 |
|---|---|---|---|---|---|---|---|---|
| 1 | 3.816 | 53.819 | -179.208 | 175.530 | 69.642 | -69.141 | -57.790 | 118.298 |
| 5 | 3.914 | -53.349 | -179.235 | -174.387 | 53.690 | 65.619 | -74.182 | -62.194 |
| 11 | 4.355 | 68.154 | 179.994 | -176.450 | -83.299 | 58.526 | 53.550 | -141.706 |
| 15 | 4.562 | 61.258 | -170.271 | 177.242 | -44.333 | -57.577 | 174.407 | -75.345 |
| 19 | 4.629 | 55.777 | -178.960 | 176.003 | -52.861 | -69.909 | 68.291 | 60.876 |
| 23 | 4.717 | -174.507 | 176.995 | -177.748 | 49.431 | 57.949 | -81.919 | 117.145 |
| 25 | 4.746 | -58.189 | 177.777 | -176.697 | -72.215 | 63.896 | 55.668 | -125.503 |
| 31 | 4.894 | -60.642 | -77.201 | 174.886 | -67.754 | -83.133 | 69.619 | 75.700 |
| 35 | 4.915 | 60.197 | 178.496 | -176.529 | -73.639 | 65.007 | 55.944 | -127.773 |
| 37 | 4.964 | -58.822 | 173.654 | -63.368 | -56.005 | 157.852 | -69.364 | -69.730 |
| 38 | 4.967 | -80.554 | 68.159 | 172.974 | 57.084 | 68.307 | -80.198 | -64.593 |
| 41 | 5.075 | 68.049 | -173.473 | 70.735 | 45.051 | 58.260 | -82.603 | -64.341 |

Table 1 (*continued*)

| | | | | | | | | |
|---|---|---|---|---|---|---|---|---|
| 42 | 5.080 | 56.697 | -178.889 | 175.782 | 60.462 | -138.804 | 65.284 | 65.286 |
| 43 | 5.080 | 67.919 | -173.555 | 70.559 | 45.179 | 58.404 | -82.231 | 116.256 |
| 44 | 5.082 | 63.347 | -176.579 | 178.915 | -66.368 | 127.861 | -69.667 | 103.995 |
| 45 | 5.083 | 63.282 | -176.685 | 178.856 | -66.353 | 127.823 | -69.312 | -76.431 |
| 46 | 5.087 | 57.057 | -179.119 | 175.761 | 60.510 | -137.959 | 65.510 | -112.785 |
| 49 | 5.148 | 67.536 | -173.504 | 70.655 | 45.246 | 58.329 | -82.223 | -63.956 |
| 50 | 5.154 | 67.563 | -173.626 | 70.588 | 45.203 | 58.418 | -82.138 | 115.973 |
| 54 | 5.168 | 61.623 | -172.551 | -179.953 | -49.180 | 89.799 | -165.509 | 109.842 |
| 56 | 5.213 | -52.338 | 173.797 | -172.163 | 48.633 | 60.135 | -171.556 | -78.396 |
| 58 | 5.224 | -64.429 | -175.782 | 177.967 | -49.497 | -58.141 | 82.074 | 63.874 |
| 59 | 5.225 | -174.743 | 175.354 | -177.238 | -53.593 | -62.807 | 84.147 | -114.932 |
| 64 | 5.264 | -64.981 | -175.520 | 177.714 | -49.123 | -57.773 | 83.155 | -116.894 |
| 68 | 5.302 | -56.070 | 177.437 | -172.138 | 53.660 | 70.158 | -71.447 | -59.475 |
| 69 | 5.324 | 60.470 | -179.140 | -179.977 | 60.636 | 179.660 | 62.919 | 73.789 |
| 73 | 5.359 | 60.970 | -179.752 | -178.973 | 60.461 | -179.576 | 179.574 | 91.820 |
| 74 | 5.363 | 62.791 | -169.476 | 175.503 | -42.432 | -57.180 | 174.893 | 105.039 |
| 77 | 5.418 | 59.676 | -177.380 | -179.649 | -61.897 | -178.851 | -179.479 | -92.625 |
| 80 | 5.449 | 59.736 | -179.165 | -179.823 | 60.623 | -179.449 | 63.286 | 73.269 |
| 84 | 5.463 | 60.821 | -171.358 | 179.476 | -48.428 | 89.917 | -165.254 | -66.707 |
| 86 | 5.473 | 73.671 | 176.062 | -172.521 | -51.975 | -62.369 | 83.220 | 65.863 |
| 88 | 5.482 | 60.659 | -179.164 | -179.100 | 61.039 | -178.161 | -63.263 | -76.261 |
| 89 | 5.484 | -58.309 | 178.368 | -177.776 | 73.292 | -66.837 | -59.063 | 118.370 |
| 90 | 5.484 | 59.870 | -177.633 | -179.400 | -62.220 | -177.565 | -63.008 | -74.652 |
| 91 | 5.486 | -59.782 | 177.930 | 179.709 | 62.433 | 178.738 | 179.678 | -87.868 |
| 94 | 5.493 | -85.386 | 63.275 | 177.353 | 59.454 | 76.257 | -76.249 | -68.174 |
| 100 | 5.538 | 60.242 | -177.634 | -179.191 | -62.446 | -179.965 | 63.615 | 75.688 |

E – AMBER energy (kcal/mol); see Fig 1 for dihedrals' notation: D1 – $O_1$-$C_2$-$C_{11}$-$N_{12}$, D2 – $C_2$-$C_{11}$-$N_{12}$-$C_{13}$, D3 – $C_{11}$-$N_{12}$-$C_{13}$-$C_{14}$, D4 – $N_{12}$-$C_{13}$-$C_{14}$-$C_{15}$, D5 – $C_{13}$-$C_{14}$-$C_{15}$-$C_{16}$, D6 – $C_{14}$-$C_{15}$-$C_{16}$-$C_{17}$ and D7 – $C_{15}$-$C_{16}$-$C_{17}$-$C_{18}$

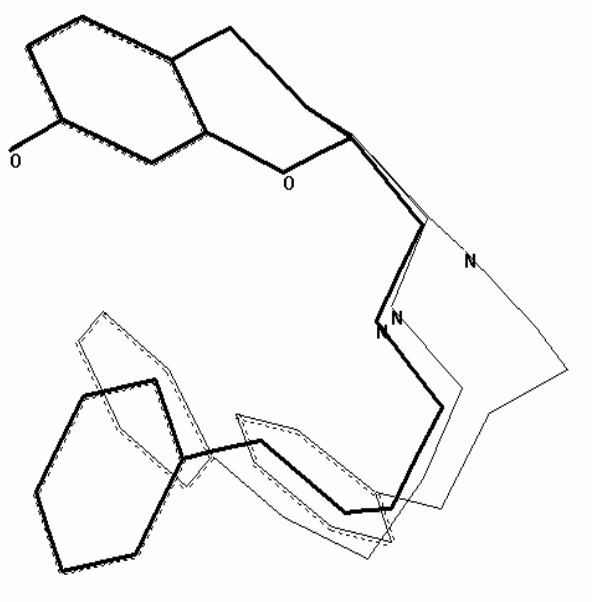


Fig. 2 – Superposition of three AMBER conformers with energies in a thermal energy range of 0-0.5 kcal above the energy of the most stable conformer (thick lines).

Optimization with AM1 semiempirical MO method of the geometries presented in Table 1 resulted in the same number of conformers, but they are spread on a larger energy range (ΔHf is between -62.008 and -56.773 kcal/mol) as can be seen from results depicted in Table 2, where conformers are ordered in the ascending order of their formation energy. The order of AMBER conformers according to their energy is modified for the AM1 conformers.

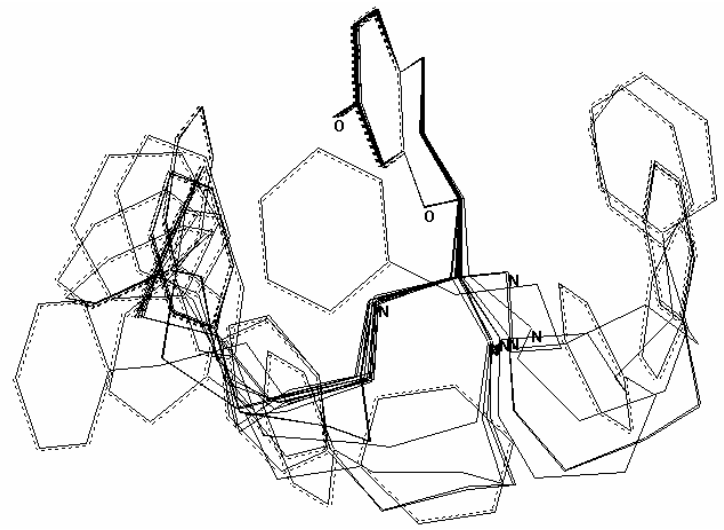


Fig. 3 – Superposition of 27 AMBER conformers with energies in a range of 1.5 kcal above the energy of the most stable conformer.

*Table 2*

Heat of formation, dipole moment and dihedral values for 100 lowest energy conformers resulted from geometry optimization with AM1 method

| No | ΔHf | DM | D1 | D2 | D3 | D4 | D5 | D6 | D7 |
|---|---|---|---|---|---|---|---|---|---|
| 39 | -62.008 | 2.154 | -68.290 | 173.507 | -69.412 | -61.004 | -172.753 | -70.483 | -65.345 |
| 92 | -61.931 | 2.308 | -69.751 | 170.009 | -172.421 | 72.238 | 174.061 | 177.875 | -72.851 |
| 95 | -61.694 | 1.743 | 65.871 | -167.150 | 172.872 | -71.808 | -173.600 | -177.671 | 72.797 |
| 62 | -61.646 | 2.619 | -66.945 | 84.210 | -163.583 | 70.833 | 64.561 | 171.811 | 74.805 |
| 78 | -61.494 | 1.636 | 65.137 | -169.129 | 167.432 | 65.025 | 176.377 | 177.807 | -70.926 |
| 71 | -61.022 | 2.374 | -68.269 | 157.843 | -162.123 | 63.931 | 66.363 | -169.339 | 72.511 |
| 100 | -60.996 | 1.658 | 65.412 | -170.762 | 170.267 | -73.119 | -171.728 | 72.081 | 73.667 |
| 83 | -60.964 | 1.751 | 65.819 | -168.695 | 165.806 | -77.955 | 177.122 | -76.681 | -78.261 |
| 48 | -60.947 | 3.096 | 47.058 | 76.367 | -113.494 | -71.684 | -175.238 | 72.118 | 73.044 |
| 84 | -60.927 | 1.839 | 66.099 | -167.355 | 174.546 | -67.334 | 106.054 | 178.949 | -74.273 |
| 47 | -60.914 | 3.040 | 42.895 | 72.571 | -106.138 | -75.442 | -175.826 | 72.001 | 75.413 |
| 97 | -60.885 | 3.214 | -62.593 | -72.661 | 170.552 | 64.578 | -100.650 | -69.801 | -74.951 |
| 88 | -60.829 | 1.778 | 64.866 | -167.112 | 167.284 | 64.946 | -174.330 | -72.345 | -70.795 |
| 98 | -60.829 | 1.779 | 64.840 | -167.025 | 167.281 | 64.991 | 174.375 | -72.339 | -70.954 |
| 18 | -60.771 | 1.905 | 63.491 | -155.400 | 157.798 | -65.405 | -67.396 | 170.839 | -70.577 |
| 15 | -60.769 | 1.896 | 63.529 | -156.155 | 157.071 | -64.843 | -66.498 | 171.133 | -70.691 |
| 93 | -60.755 | 1.555 | 66.482 | -167.244 | 171.843 | -72.897 | -174.478 | -72.482 | -68.674 |
| 61 | -60.739 | 1.883 | 62.416 | -164.265 | 161.601 | -65.388 | 106.479 | -167.003 | 82.525 |
| 45 | -60.719 | 1.536 | 65.405 | -168.906 | 165.139 | -77.807 | 178.121 | -76.221 | -75.682 |
| 53 | -60.677 | 1.733 | 66.248 | -167.516 | 168.376 | 65.972 | 178.254 | 73.519 | 70.378 |
| 82 | -60.665 | 1.748 | 65.226 | -170.262 | 165.150 | 62.964 | 175.468 | 71.242 | 66.692 |
| 42 | -60.649 | 1.724 | 65.790 | -167.492 | 166.792 | 65.492 | 179.648 | 73.620 | 79.248 |
| 54 | -60.635 | 1.819 | 64.744 | -165.169 | 170.411 | -65.747 | 106.006 | -172.184 | 78.797 |
| 58 | -60.519 | 2.813 | -62.553 | -73.566 | 172.239 | -77.415 | -100.111 | 73.214 | 69.129 |
| 31 | -60.514 | 2.830 | -63.888 | -75.310 | 172.515 | -79.583 | -92.288 | 78.721 | 70.716 |
| 43 | -60.296 | 1.485 | 65.963 | -168.466 | 71.738 | 70.916 | 73.649 | -95.222 | -64.309 |
| 27 | -59.938 | 1.757 | 65.288 | -171.182 | 146.983 | -93.953 | 71.880 | 64.165 | 57.666 |
| 29 | -59.888 | 2.445 | -68.198 | 171.325 | -163.648 | -66.672 | 95.158 | 65.137 | 76.239 |
| 5 | -59.707 | 1.968 | -69.287 | 172.731 | -170.245 | 77.631 | 77.228 | -89.786 | -64.191 |
| 4 | -59.680 | 1.810 | 65.984 | -166.937 | 168.738 | 70.231 | -91.811 | -66.152 | -77.541 |
| 13 | -59.490 | 1.632 | 65.475 | -169.806 | 154.191 | -95.485 | 70.266 | 63.109 | 55.662 |
| 34 | -59.470 | 1.464 | 66.370 | -171.006 | 172.970 | -77.593 | -77.548 | 90.231 | 65.073 |
| 87 | -59.362 | 1.521 | 65.369 | -163.195 | 174.390 | -75.051 | -73.892 | 91.137 | 61.990 |
| 24 | -58.526 | 1.729 | -166.290 | 179.690 | -175.170 | 76.969 | 70.746 | -99.996 | -64.272 |
| 66 | -58.419 | 2.741 | -164.204 | 178.783 | 174.216 | -76.181 | -69.978 | 100.594 | 64.274 |
| 99 | -58.170 | 3.488 | 75.586 | -179.292 | -169.786 | -65.462 | -75.723 | 178.271 | -72.107 |
| 94 | -57.332 | 1.867 | -84.204 | 60.891 | 162.936 | 70.504 | 86.010 | -85.804 | -69.625 |
| 68 | -56.774 | 3.228 | -76.225 | -173.957 | 177.385 | 71.819 | 88.125 | -75.970 | -61.663 |

ΔHf – heat of formation (kcal/mol), DM – dipole moment (Debye), for the significance of the dihedrals see footnote of Table 1.

The distribution of conformers above the lowest energy conformer, **39,** is the following: four conformers are in the range of thermal energy (0 – 0.5 kcal/mol), six conformers are in the range of 1 kcal/mol, 24 conformers are in a range of 1.5 kcal/mol, 26 conformers are in a range of 2 kcal/mol, and 31 conformers are in a range of 2.5 kcal/mol above the lowest energy conformer and all (38) conformers are distributed in a range of 5.24 kcal/mol.

Comparing Fig 2 and Fig 4, displaying the superposition of the AMBER and AM1 conformers in the energy domain of thermal energy, it results that the AM1 method gives a larger conformational space than AMBER does for the conformers in the same energy domain.

In Fig. 5 the superimposition of the lowest energy conformers resulted from the two methods is displayed. One can observe that he AM1 conformer has a more extended conformation than that of the AMBER conformer. As can be seen in Table 3 the lowest energy AMBER conformer has smaller distances between unbounded atoms than the distances displayed by the lowest energy AM1 conformer distances between atoms are expressed in pm.

*Table 3*

Comparison of dihedral and distance values in the lowest energy conformers obtained with AMBER and AM1 methods

| No\dihedral | | Energy | D1 | D2 | D3 | D4 | D5 | D6 | D7 |
|---|---|---|---|---|---|---|---|---|---|
| AMBER | 1 | 3.816 | 53.819 | -179.208 | 175.530 | 69.642 | -69.141 | -57.790 | 118.298 |
| AM1 | 39 | -62.008 | -68.290 | 173.507 | -69.412 | -61.004 | -172.753 | -70.483 | -65.345 |
| No\distance | | $C_8$-$C_{11}$ | $C_8$-$N_{12}$ | $C_8$-$C_{13}$ | $C_8$-$C_{14}$ | $C_8$-$C_{15}$ | $C_8$-$C_{16}$ | $C_8$-$C_{17}$ | $C_8$-$C_{18}$ |
| AMBER | 1 | 446.4 | 472.8 | 602.2 | 653.0 | 705.6 | 620.3 | 542.1 | 405.3 |
| AM1 | 39 | 471.5 | 506.3 | 625.6 | 640.5 | 587.0 | 666.7 | 646.5 | 544.8 |

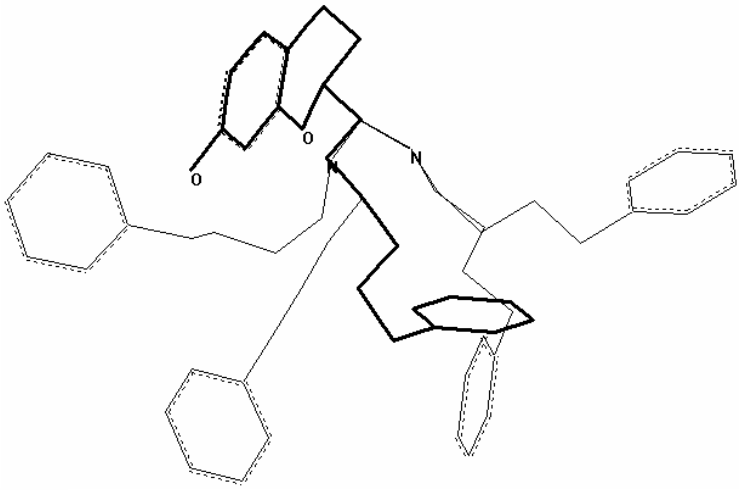


Fig. 4 – Superposition of the AM1 conformers having energies in a range of 0-0.5kcal/mol above the energy of the most stable conformer, 39 (thick line).

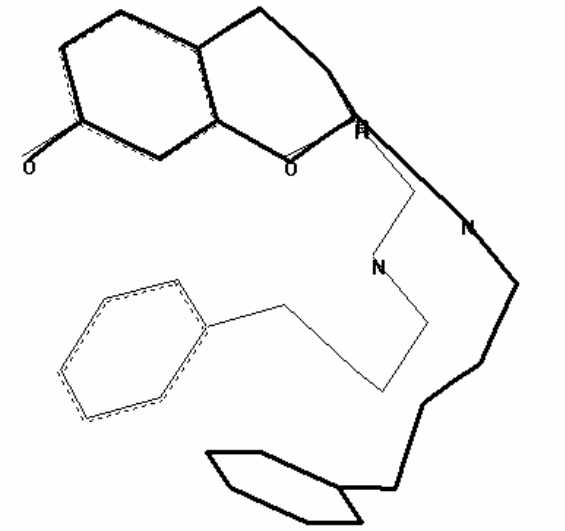


Fig. 5 – Superposition of the lowest energy conformers resulted from AMBER, conformer **1** and AM1 conformer **39** (thick line).

Values of the conformer energy suggest that a large number of conformers can populate the low energy levels on the potential energy surface and this number of conformers could be obtained from synthesis. It is interesting to find out what are the rotation energies of flexible bonds of these conformers and if these conformers could be able to surmount the rotation barriers energy for achieving other conformations more appropriate for interactions with the amino acid residues from the D2 receptor active site. In Fig. 6 the rotation barrier energies of the dihedrals: $O_1$-$C_2$-$C_{11}$-$N_{12}$, $C_{11}$-$N_{12}$-$C_{13}$-$C_{14}$, $N_{12}$-$C_{13}$-$C_{14}$-$C_{15}$, $C_{14}$-$C_{15}$-$C_{16}$-$C_{17}$, and $C_{15}$-$C_{16}$-$C_{17}$-$C_{18}$ are displayed. Rotation of the $C_2$-$C_{11}$, and $C_{15}$-$C_{16}$ bonds needs energies lower than 8 kcal/mol, while rotation of the $C_{11}$-$N_{12}$, $C_{13}$-$C_{14}$, and $C_{16}$-$C_{17}$ bonds (corresponding to the $N_{12}$-$C_{13}$-$C_{14}$-$C_{15}$, $C_{14}$-$C_{15}$-$C_{16}$-$C_{17}$, and $C_{15}$-$C_{16}$ $C_{15}$-$C_{16}$-$C_{17}$-$C_{18}$ dihedrals) needs energies over 15 kcal/mol.

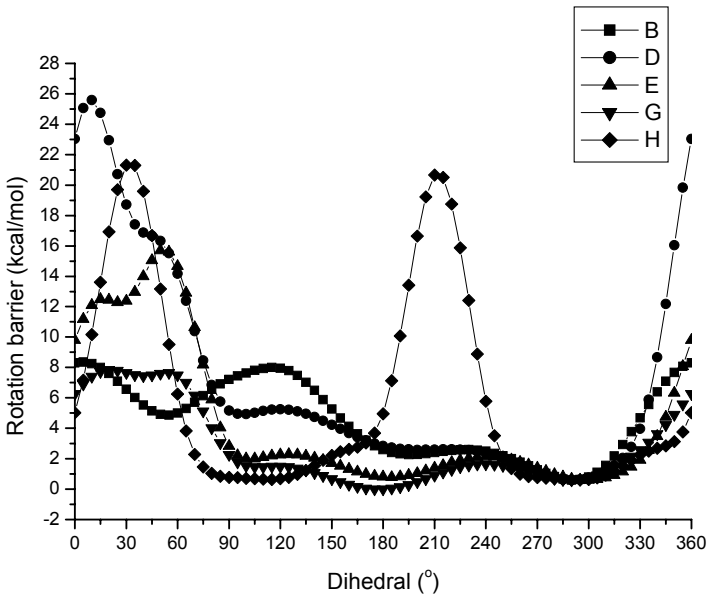


Fig. 6 – Rotation barriers for dihedrals of the lowest energy conformer obtained from conformational search using the AM1 method. Notation of dihedrals in the legend is: B – $O_1$-$C_2$-$C_{11}$-$N_{12}$, D – $C_{11}$-$N_{12}$-$C_{13}$-$C_{14}$, E – $N_{12}$-$C_{13}$-$C_{14}$-$C_{15}$, G – $C_{14}$-$C_{15}$-$C_{16}$-$C_{17}$, H – $C_{15}$-$C_{16}$-$C_{17}$-$C_{18}$.

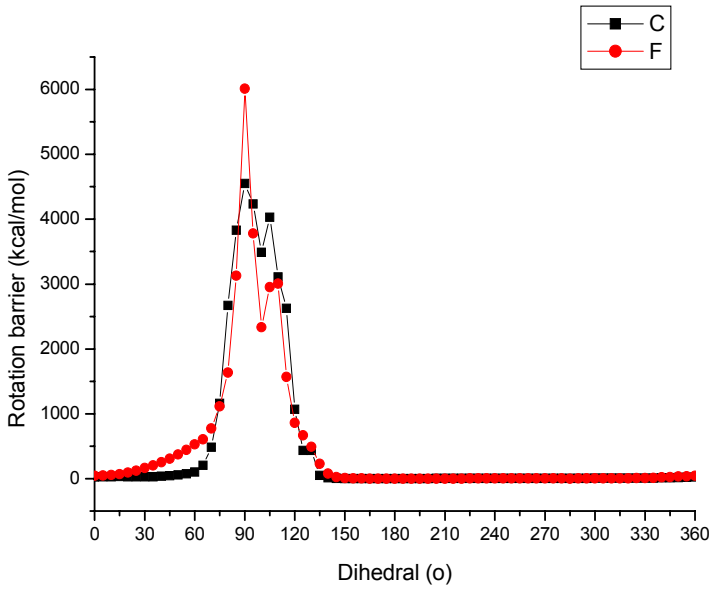


Fig. 7 – Rotation barriers for dihedrals of the lowest energy conformer obtained from conformational search using the AM1 method. Notation of dihedrals in the legend is: C for $C_2$-$C_{11}$-$N_{12}$-$C_{13}$ and F for $C_{13}$-$C_{14}$-$C_{15}$-$C_{16}$.

In Fig. 7 the rotation barrier energies of the dihedrals: $C_2$-$C_{11}$-$N_{12}$-$C_{13}$, and $C_{13}$-$C_{14}$-$C_{15}$-$C_{16}$, is displayed. The conformer energies for the $C_{11}$-$N_{12}$ and $C_{14}$-$C_{15}$ bonds are very high for the dihedral values between 60 and 120º.

The ligands of this series have been docked in the active site of a D2 receptor 3D model, constructed by homology with the X-ray structure of rhodopsin (pdb entry 1F88). We compared the active conformation of the ligand in the receptor site with the conformers obtained through conformational analysis (Fig. 8).

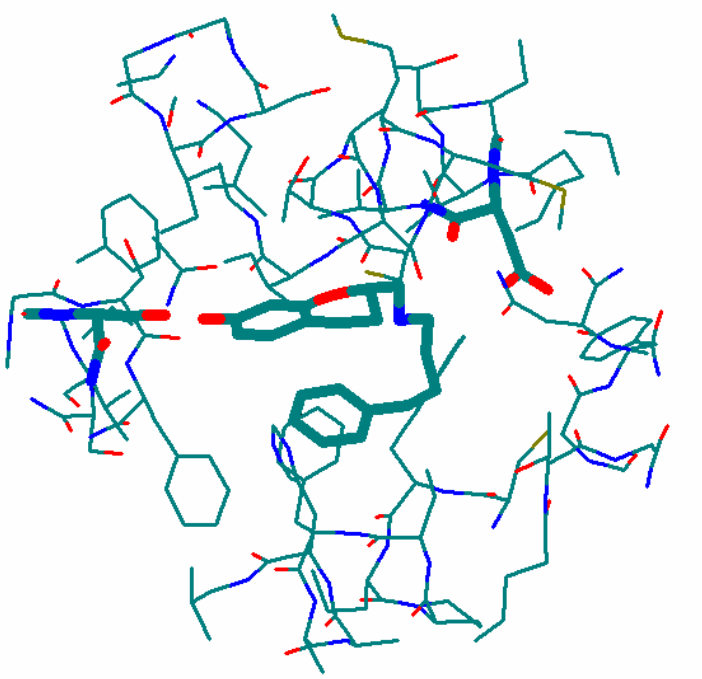

Fig. 8 – The AMBER lowest energy conformer in the D2 receptor active site.

Superposition of the lowest energy AMBER conformer on the lowest energy conformer docked in the D2 receptor active site revealed that the first one can occupy in the situs a position similar to that of the docked conformer. This observation suggests that the D2 receptor ligand binding domain is large enough to allow conformational changes of the ligand in order to achieve optimum ligand-receptor interactions.

We performed the docking of S conformers at C2 position on the chromane moiety, this leads to an interesting observation: the hydrogen bond between Ser144 and chromane OH group are not possible anymore. This observation suggests the stereoselective behaviour of the receptor interacting with the chromane derivatives.

## CONCLUSIONS

Conformational analysis of a potent ligand, 2-[(4-phenyl-butylamino)-methyl]-chroman-7-ol, acting as partial agonist on the D2 receptor showed that the conformational space occupied by the ligand is large. The AM1 conformers can be included in a parallelepiped with edges of 12.68, 12.88 and 13.97 Å respectively.

For ligands having flexible bonds, the AM1 method gives conformers in more extended conformations than those obtained with the AMBER method.

According to the small energy barriers between different conformers the ligand can adopt easily conformations suitable for interaction with residues from the D2 receptor ligand binding domain.

The active site of the D2 receptor is large enough to allow conformational changes of the ligand in order to achieve the optimum ligand-receptor interactions.

Docking studies revealed that D2 receptor had a stereoselective behaviour, preferring (2R)-chromane derivatives.

## REFERENCES

1. Seeman P, Ohara K, Ulpian C, Seeman MV, Jellinger K, Tol HH, Niznik HB, *Neuropsychopharmacology* **1993,** *8*, 137-142.

2. McCaul M, Turkhan JS, Stitzer ML, *Alcoholism: Clinic Exp Res* **1989,** *13***,** 613–635.
3. Wadenberg M-L, Salmi P, Jimenez P, Svensson T, Ahlenius S, *Eur Neuropsychopharmacol* **1996,** *6*, 305-310.
4. Mewshaw RE, Kavanagh J, Stack G, Marquis KL, Shi X, Kagan MZ, Webb MB, Katz AH, Park A, Kang YH, Abou-Gharbia M, Scerni R, Wasik T, Cortes-Burgos L, Spangler T, Brennan J.A, Piesla M, Mazandarani H, Cockett MI, Ochalski R, Coupet J, Andree TH, *J.Med.Chem.* **1997,** *40*, 4235-4256.
5. Dewar M, Zoebisch EG, Healy EF, Stewart JJP, *J. Am. Chem. Soc*., **1985**, *107***,** 3902-3909.
6. HyperChem$^{TM}$, Release 7.52 for Windows, Hypercube, Inc.

*Revue Roumaine de Chimie*, **2007**, *52*(8–9), 845–851

*Dedicated to Professor Victor-Emanuel Sahini on the occasion of his 80th anniversary*

# QSAR STUDY FOR A SERIES OF IMIDAZO[1,5-*A*]-QUINOXALINE AND PYRAZOLO[1,5-C]QUINAZOLINE DERIVATIVES ACTING ON $GABA_A$/BENZODIAZEPINE RECEPTOR

Ramona RAD, Maria MRACEC*, Liliana OSTOPOVICI, Ana BOROTA, Mircea MRACEC

Roumanian Academy, Institute of Chemistry Timişoara, 24, M.Viteazul Bd., 300223-Roumania
e-mail: mmracec@acad-icht.tm.edu.ro

*Received May 29, 2007*

Some classical QSARs on a large series of 4,5-dihydro-imidazo[1,5-*a*]quinoxaline and pyrazolo[1,5-c]quinazolines derivatives acting at $GABA_A$/benzodiazepine receptor are presented. The MTD method has been applied and the MTD descriptor has been used together with other descriptors in MLR models. The best model includes ten descriptors: one Galvez topological charge index, seven BCUT descriptors mediated on atomic polarizabilities or on Sanderson atomic electronegativities and two 2D autocorrelation descriptors. This model sugests that the quinoxaline and quinazoline derivatives could interact with amino acids residues of the receptor by electrostatic or charge transfer processes.

## INTRODUCTION

Since 1960 benzodiazepines that act as agonists at the $GABA_A$/benzodiazepine receptor have been used clinically for their anxiolytic, sedative and anticonvulsive effects. The disadvantages of these drugs consist in difficulty to separate these actions which, in time, lead to various side effects such as ataxia and amnesic-like effects, ethanol and barbiturate potentiation, sedation, as well as tolerance and dependence. There has been some extensive structure–activity studies aimed for developing new potent ligands having lower side effects, acting on $GABA_A$/benzodiazepine receptor. The aim of this work was to obtain quantitative structure-activity relationships in order to evidence the structural properties of quinoxaline and quinazoline derivatives that influence significantly their biological activity at the $GABA_A$/benzodiazepine receptor.

## METHODS

Structure and biological activities determined by Carter et all[1-3] for 128 of 4,5-dihydro-imidazo[1,5-*a*]quinoxaline and pyrazolo[1,5-c]quinazolines derivatives have been used to obtain regressional models between the biological activity (expressed as the reciprocal logarithm of inhibition constant, pKi) and minimum topological difference, MTD, and some other descriptors. Backbone structures are presented in Scheme 1.

Molecular geometries of 4,5-dihydro-imidazo[1,5-*a*]quinoxaline and pyrazolo[1,5-c]quinazolines derivatives have been optimized using the AMBER99 force field and then the AM1 Hamiltonian.[4] Optimizations were performed using the Polak-Ribiere conjugate gradient algorithm. All methods are implemented in HyperChem7.52.[5] Geometry was optimized till the RMS gradient was equal to or less than 0.01 kcal/Åmol. For some representative structures a conformational search has been carried out using the Conformational Search module from Hyperchem7.52.

MTD method[6,7] is based on the hypothesis that a potent ligand fits into the receptor site as a key in its lock. Such a ligand should have the complementary shape of the receptor site. MTD method defines the minimum topological difference between a "standard" (a good model of

* Corresponding author: mracic@acad-icht.tm.edu.ro

a high active ligand) and each compound from the series. The less the MTD value is, the better the activity is. In order to calculate the MTD values, a hypermolecule is built through maximum atom by atom superposition of the i = 1 ... N molecules from the series. Hypermolecule contains a number j = 1 ... M of vertices. A vertex is composed from all superposed atoms which are placed at a distance no greater than 0.5 A. In hypermolecule, for each vertex a vector $\varepsilon_j$ and an index $x_{ij}$ are assigned. The $\varepsilon_j$ vector can take the values 1 (detrimental vertices), 0 (irrelevant vertices) or -1 (beneficial vertices). The $x_{ij}$ index represents the occupancy of the j hypermolecule vertices by the atoms of the "$i^{th}$ "molecule. It can take two values $x_{ij}$ = 1 for occupied and $x_{ij}$ = 0 for unoccupied vertices. $MTD_i$, the MTD value for the "$i^{th}$ "molecule from the series is calculated using the equation:

$$MTD_i = s + \sum_{j=1}^{M} \varepsilon_j x_{ij} \quad (1)$$

where *s* represents the number of vertices with $\varepsilon_j$ = -1 of a "standard" molecule; this can be the most active compound or a generic molecule which contains predominantly atoms or groups of atoms from the most active structures. The assignment of $\varepsilon_j$ values is a cyclic process that ends when the best correlation coefficient is obtained for the equation:

$$A_i = a + a_1X_{i1} + a_2X_{i2} + \ldots - b\ MTD_i \quad (2)$$

$X_{i1}$, $X_{i2}$, ... are other descriptors, the 'a' and 'b' values are the regression coefficients.

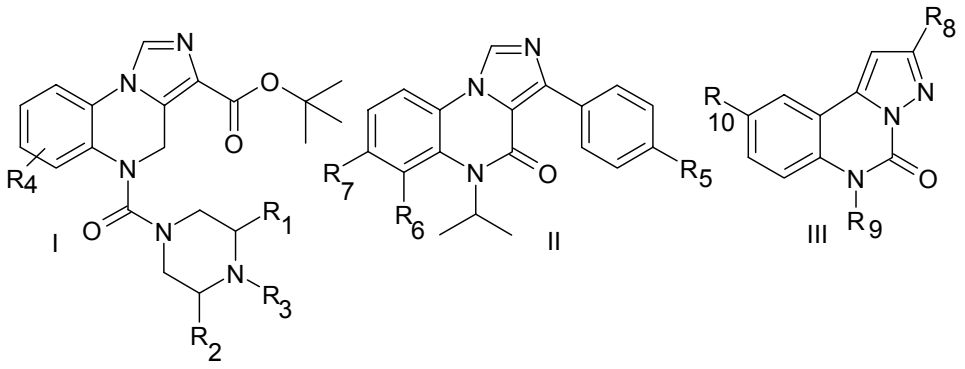


Scheme 1. Backbone structures of the quinozaline and quinazoline derivatives.

A hypermolecule (Fig 1) with *j*=78 vertices was obtained through atom by atom maximum superposition of molecules. After the building of the hypermolecule, the initial set of 128 quinoxaline and quinazoline derivatives was split in learning (99 compounds) and test sets (29 compounds). The splitting was performed manually by randomly choosing (for the test set) compounds having biological activities as diverse as possible, so that the distribution of compounds in the learning and test sets to be as similar as possible. In order to check the stability of data set, two different splittings have been carried out. Figures 1 and 2 display the distribution of compounds in the pair of test sets. As one can see the first test set has a worse distribution than the second test set.

Applying MTD method, the MTD descriptors have been calculated and they have been used in different multiple linear regressions (MLR). Apart of MTD, a number of descriptors have been calculated with the QSAR properties module from HyperChem7.52 and DRAGON3.0 softwares.[8] From the AM1 method the energies of the highest occupied molecular orbital, $E_{HOMO}$ and of the lowest unoccupied molecular orbital $E_{LUMO}$, total dipole moment and sp hybridization component of dipole moment have been calculated. Also, absolute electronegativity ($\chi$) and chemical hardness ($\eta$) have been calculated as $\chi \approx (IP + EA)/2$ and $\eta \approx (IP - EA)/2$ assuming that ionization potential, $IP \approx -E_{HOMO}$ and electron affinity, $EA \approx -E_{LUMO}$.[9,10] From AM1 method resulted also a thermodynamic property, energy of formation, $\Delta H_f$. Also, as descriptors have been tested energy terms (bond, angle, torsion and van der Waals energies) resulted for geometries of conformers optimized with the AMBER99 force field. In order to select variables the forward and backward methods from STATISTICA5.0[11] have been applied.

## RESULTS

In order to apply the MTD method seven starting receptor maps have been built, where the

assignment of vertices was done assuming that the beneficial vertices should be present especially in the highest active compounds and the detrimental vertices should be present mainly in the lowest active compounds. The optimized receptor map that gave the best correlation coefficient was:

$$S^* \begin{cases} \varepsilon_j = -1:3-10,13,15,16,22,44,54,58,63,66,67 \\ \varepsilon_j = 0:14,17,19-2,23,25,27,29-31,34-43,45-51,57,59, \\ \varepsilon_j = 1:1,2,11,12,18,24,26,28,32,33,52,53,55,56,60-62,64,68-78 \end{cases}$$

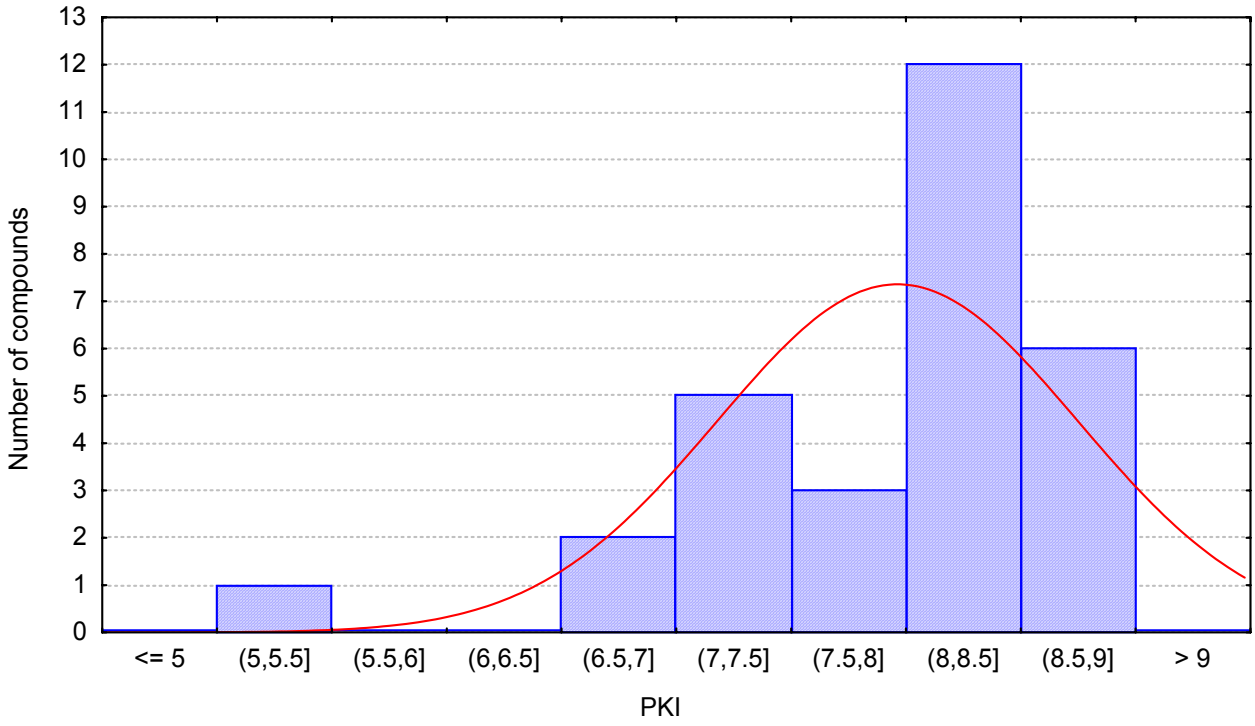


Fig. 1 – Distribution of the compounds from the first test set against their biological activity, pKi.

This map, S*, resulted for the second learning set, was used to calculate the MTD values for both sets of compounds from the first and second learning set and for the two test sets associated with the learning sets. The MTD models obtained with this map are significant, but very modest. The MTD regression model for the first learning set is:

$$pKi = 17.1429(\pm 0.6784) - 0.4623(0.0327)\ MTD \quad (3)$$

$$n = 99 \quad r = 0.821 \quad s = 0.524 \quad F = 200.16 \quad r^2_{cv} = 0.502 \quad press = 40.61$$

and the MTD regression model for the second learning set is:

$$pKi = 15.5463\ (\pm 0.481365) - 5072\ (0.030865)\ MTD \quad (4)$$

$$n = 99 \quad r = 0.858 \quad s = 0.454 \quad F = 270.04 \quad r^2_{cv} = 0.645 \quad press = 26.91$$

Using the regresions (3) and (4) the pKi values of the test sets have been calculated. The pKi calculated values, the experimental pKi values and the differences between them for the compounds from the two test sets are displayed in Table 1. Although the differences obtained with the regression (4) are slightly better than those obtained with regression (3), for some compounds the differences are over one logarihtm unit. Given that the standard error of estimate was 0.524 and 0.454, respectively for the regressions (3) and (4) these results were expectable.

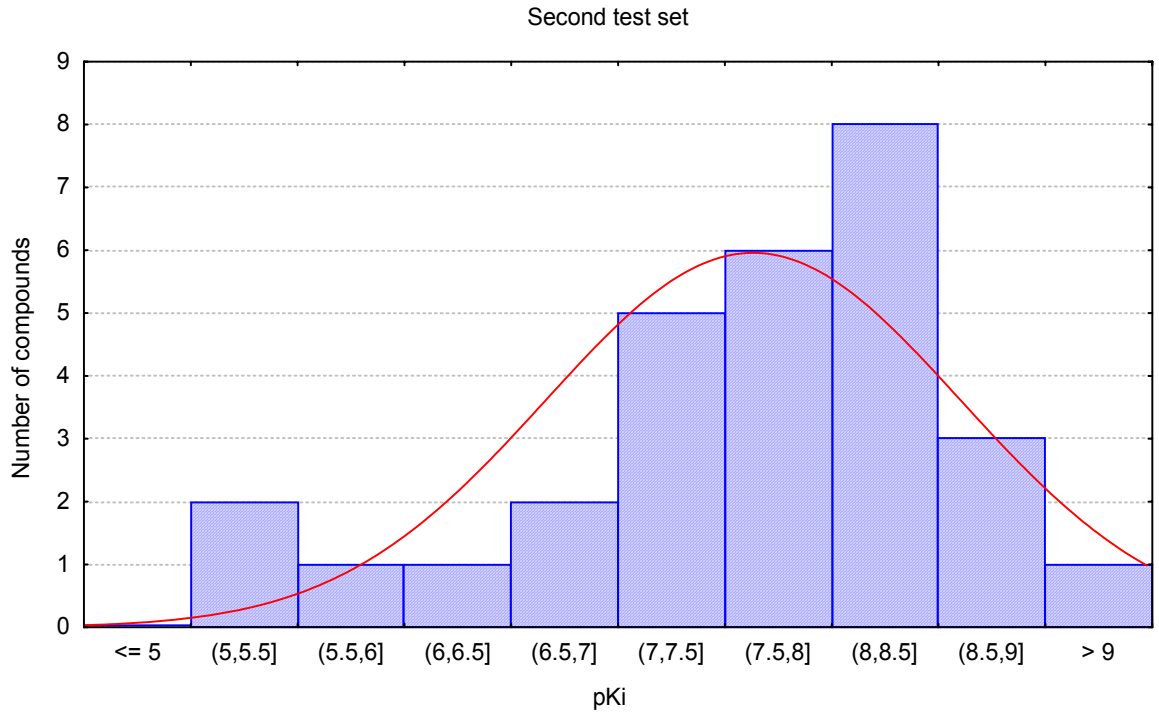


Fig. 2 – Distribution of compounds from the second test set against their biological activity, pKi.

*Table 1*

pKi values calculated with regressions (3) and (4)

| First test set; pKi calculated with eqn. (3) | | | | | Second test set; pKi calculated with eqn. (4) | | | | |
|---|---|---|---|---|---|---|---|---|---|
| No | MTD | pKi exp | pKi calc | Diff | No | MTD | pKi exp | pKicalc | Diff |
| 2 | 21 | 8.517 | 7.435 | 1.082 | 1 | 14 | 8.386 | 8.448 | -0.062 |
| 3 | 22 | 8.176 | 6.972 | 1.204 | 7 | 14 | 7.964 | 8.448 | -0.484 |
| 8 | 20 | 8.485 | 7.897 | 0.588 | 13 | 14 | 8.332 | 8.448 | -0.116 |
| 9 | 21 | 8.349 | 7.435 | 0.914 | 14 | 14 | 8.022 | 8.448 | -0.426 |
| 11 | 23 | 7.250 | 6.51 | 0.740 | 22 | 14 | 8.870 | 8.448 | 0.422 |
| 13 | 20 | 8.332 | 7.897 | 0.435 | 51 | 14 | 8.225 | 8.448 | -0.223 |
| 14 | 21 | 8.022 | 7.435 | 0.587 | 53 | 14 | 7.747 | 8.448 | -0.701 |
| 15 | 22 | 6.602 | 6.972 | -0.370 | 54 | 14 | 8.262 | 8.448 | -0.186 |
| 19 | 23 | 7.700 | 6.51 | 1.190 | 56 | 14 | 8.287 | 8.448 | -0.161 |
| 20 | 23 | 7.401 | 6.51 | 0.891 | 69 | 18 | 7.402 | 6.42 | 0.982 |
| 21 | 22 | 8.280 | 6.972 | 1.308 | 72 | 17 | 5.772 | 6.927 | -1.155 |
| 24 | 21 | 8.255 | 7.435 | 0.820 | 74 | 18 | 7.836 | 6.42 | 1.416 |
| 47 | 20 | 7.521 | 7.897 | -0.376 | 78 | 16 | 8.467 | 7.434 | 1.033 |
| 61 | 25 | 7.415 | 5.585 | 1.830 | 79 | 15 | 8.529 | 7.941 | 0.588 |
| 62 | 23 | 7.499 | 6.51 | 0.989 | 80 | 15 | 7.955 | 7.941 | 0.014 |
| 65 | 24 | 6.939 | 6.048 | 0.891 | 82 | 13 | 9.013 | 8.955 | 0.058 |
| 78 | 22 | 8.467 | 6.972 | 1.495 | 87 | 15 | 8.783 | 7.941 | 0.842 |
| 79 | 21 | 8.529 | 7.435 | 1.094 | 88 | 17 | 6.666 | 6.927 | -0.261 |
| 80 | 21 | 7.955 | 7.435 | 0.520 | 89 | 17 | 7.313 | 6.927 | 0.386 |
| 83 | 19 | 8.812 | 8.359 | 0.453 | 93 | 17 | 6.476 | 6.927 | -0.451 |
| 85 | 20 | 8.233 | 7.897 | 0.336 | 95 | 15 | 7.456 | 7.941 | -0.485 |
| 86 | 21 | 7.879 | 7.435 | 0.444 | 96 | 16 | 7.326 | 7.434 | -0.108 |
| 87 | 21 | 8.783 | 7.435 | 1.348 | 98 | 15 | 7.688 | 7.941 | -0.253 |
| 104 | 19 | 8.604 | 8.359 | 0.245 | 111 | 17 | 7.553 | 6.927 | 0.626 |
| 105 | 20 | 8.296 | 7.897 | 0.399 | 113 | 18 | 7.229 | 6.42 | 0.809 |
| 107 | 22 | 7.324 | 6.972 | 0.352 | 114 | 19 | 6.979 | 5.913 | 1.066 |
| 108 | 19 | 8.857 | 8.359 | 0.498 | 121 | 17 | 8.131 | 6.927 | 1.204 |
| 109 | 20 | 8.381 | 7.897 | 0.484 | 126 | 17 | 5.483 | 6.927 | -1.444 |
| 128 | 23 | 5.182 | 6.51 | -1.328 | 128 | 18 | 5.182 | 6.42 | -1.238 |

Seven compounds, 13,14,78-80,87,128 belong to both test sets. Comparing their differences (pKi exp – pKi calc, exhibited in columns Diff) one can observe that the diferences for the compounds in the second test set are slightly lower than those of the compounds from the first test set, however globally, the results of the regression (4) are also very modest. In order to obtain better statistical models the MTD descriptor was associated with other partner descriptors. The indices of different statistical significant models (obtained with the first learning set) are collected in Table 2.

*Table 2*

Statistical parameters for some significant multiple linear regression

| **Descriptors** | | **r** | **$r^2$** | **$r^2$adj** | **s** | **F** |
|---|---|---|---|---|---|---|
| MTD,logP,RDF025p,RDF055p | (3) | 0.853 | 0.727 | 0.716 | 0.486 | 62.72 |
| MTD,logP,MoR32e | (4) | 0.853 | 0.728 | 0.720 | 0.483 | 84.92 |
| MTD,logP,JGI1,GGI1 | (5) | 0.859 | 0.737 | 0.726 | 0.477 | 65.95 |
| MTD,logP,BELe1,BELe2,BEHp7,BELp1 | (6) | 0.872 | 0.761 | 0.745 | 0.460 | 48.84 |
| MTD,logP,HATS0v,HATS1v,HATS4v,HATS5m | (7) | 0.873 | 0.762 | 0.747 | 0.459 | 49.92 |
| MTD, MoR09m, MoR10m,MoR12m,MoR18m, MoR21m, MoR25m | (8) | 0.874 | 0.764 | 0.746 | 0.460 | 42.05 |
| MTD,logP,X2A,X0v,X1v,X0Av,X1Av | (9) | 0.875 | 0.765 | 0.747 | 0.459 | 42.31 |
| MTD,logP,HATS2p,HATS4p,HATS5p,HATS7p,H0p,RTu,R4u | (10) | 0.901 | 0.812 | 0.791 | 0.417 | 38.05 |

Log P – log 1-octanol/water partition coefficient calculated with QSAR properties module from HyperChem7.52; piPC04 – molecular multiple path count of order 04; RDF025p – radial distribution function -2.5 / weighted by atomic polarizabilities; RDF055p – radial distribution function -5.5 / weighted by atomic polarizabilities; MoR32e – 3D-MoRSE - signal 32 / weighted by atomic Sanderson electronegativities; JGI1 – mean topological charge index of order 1; GGI1 – topological charge index of order 1; BELe1 – lowest eigenvalue n. 1 of Burden matrix / weighted by atomic Sanderson electronegativities; BELe2 – lowest eigenvalue n. 2 of Burden matrix / weighted by atomic Sanderson electronegativities; BEHp7 – highest eigenvalue n. 7 of Burden matrix / weighted by atomic polarizabilities; BELp1 lowest eigenvalue n. 1 of Burden matrix/weighted by atomic polarizabilities; HATS0v – leverage-weighted autocorrelation of lag 0 / weighted by atomic van der Waals volumes; HATS1v – leverage-weighted autocorrelation of lag 1 / weighted by atomic van der Waals volumes; HATS4v – leverage-weighted autocorrelation of lag 4 / weighted by atomic van der Waals volumes; HATS5m – leverage-weighted autocorrelation of lag 5 / weighted by atomic masses; MoR09m – 3D-MoRSE - signal 09 / weighted by atomic masses; MoR010m –3D-MoRSE - signal 10 / weighted by atomic masses; MoR12m – 3D-MoRSE signal 12 / weighted by atomic masses; MoR18m – 3D-MoRSE - signal 18 / weighted by atomic masses; MoR21m – 3D-MoRSE - signal 21 / weighted by atomic masses; MoR25m – 3D-MoRSE - signal 25 / weighted by atomic masses; X2A – average connectivity index chi-2; X0v – valence connectivity index chi-0; X1v – valence connectivity index chi-1; X0Av – average valence connectivity index chi-0; X1Av – average valence connectivity index chi-1; HATS2p leverage-weighted autocorrelation of lag 2 / weighted by atomic polarizabilities; HATS4p – leverage-weighted autocorrelation of lag 4 / weighted by atomic polarizabilities; HATS5p – leverage-weighted autocorrelation of lag 5 / weighted by atomic polarizabilities; HATS7p – leverage-weighted autocorrelation of lag 7 / weighted by atomic polarizabilities; H0p – H autocorrelation of lag 0 / weighted by atomic polarizabilities; RTu – R total index / unweighted; R4u – R autocorrelation of lag 4 / unweighted.

Even if the regresions from Table 2 also have low statistical indices, but the descriptors included in the models could give some information regarding the importance of various structural properties for the biological activity of quinoxaline and quinazoline derivatives. For example, logP is present in almost all models sugesting that the ligand hydrophobicity influences in a certain degree the pKi values. The presence of descriptors weighted on atomic polarizabilities or atomic electronegativities Sanderson such as: radial distribution function, BCUT, GETAWAY descriptors could signify that pKi is influenced by electronic or electrostatic properties of the compounds.

Because the MTD has a high partial correlation coefficient there are only few tolerated descriptors as partner descriptors. The higher the MTD partial correlation coefficient is, the fewer MTD partner descriptors are. Therefore for the second learning set the best obtained correlation had 0.89 for the total correlation coefficient. In these cases, besides steric information, MTD descriptor contains hydrophobicity and electronic information. Its steric nature is covered by other effects.

In order to obtain other models with better statistical indices we used a set of descriptors provided by DRAGON3.0. The outliers were eliminated and the following regression was obtained:

$$pKi = 95.8351(\pm10.101) + 3.052353(\pm0..61579)\ BELm6 - 3.356161(\pm0.3067)BEHv8 - 71.29569(\pm3.970161)BELv3 + 9.463132(\pm0.725744)BEHe4 - 47.8192(\pm4.820646)BELe1 + 42.05471(\pm4.48708)BEHp1 + 73.1973(\pm3.94718)BELp3 - 3.953559(\pm0.295809)GGI7 + 0.047589(\pm0.005007)ATS8e - 0.108897(\pm0.010495)ATS7p \quad (5)$$

$$n = 83\ \ r = 0.962\ \ r^2 = 0.925\ \ r^2_{adj} = 0.915\ \ s = 0.197\ \ F = 89.15\ \ press = 2.80$$

To verify the reliability of this regressional model the calculated pKi values against the experimental ones have been plotted. A high leverage point was observed for low pKi values. By eliminating this point (compound 106) the following model was obtained:

$$pKi = -97.1579(\pm10.4675) + 3.071(\pm0.62)\ BELm6 - 3.3509(\pm0.3084)BEHv8 - 72.7376(\pm4.8618)BELv3 + 9.5754(\pm0.7608)BEHe4 - 48.0567(\pm4.8668)BELe1 + 42.4055(\pm4.5604)BEHp1 + 74.6249(\pm4.8271)BELp3 - 3.9647(\pm0.2981)GGI7 + 0.0478(\pm0.005)ATS8e - 0.1095(\pm0.0106)ATS7p \quad (6)$$

$$n = 82\ \ r = 0.955\ \ r^2 = 0.912\ \ r^2_{adj} = 0.899\ \ s = 0.198\ \ F = 73.34\ \ press = 2.79$$

The new pKi values calculated with the regression model (6) have been plotted against the experimental pKi values. The regression line and the distribution of the points around the regression line can be seen in Fig. 3. The model obtained has good statistical parameters: the value of the standard error of estimate (s) is around 0.2 logarithm units, in the experimental errors domain.

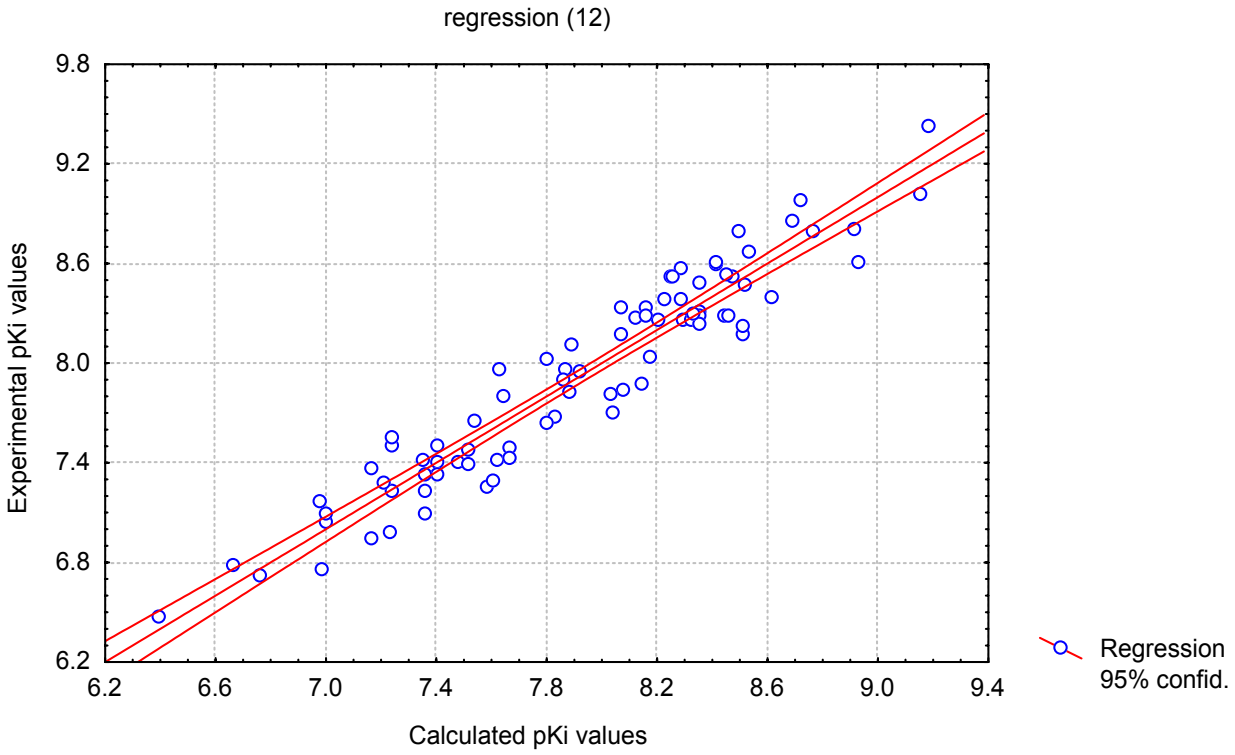


Fig. 3 – Calculated pKi against experimental pKi.

The first seven descriptors from the regression (6) are BCUT descriptors. GGI7 is Galvez topological charge index and the last two are 2D autocorrelation indices. In the BCUT group of descriptors there are three couples of descriptors weighted by: 1) atomic van der Waals volume, 2) atomic Sanderson electronegativities and 3) atomic polarizabilities. The two 2D autocorrelation indices are also weighted by atomic Sanderson electronegativities and atomic polarizabilities. Thus, the regression model (6) is similar with the models presented in Table 2 and they suggest that pKi is influenced by electronic properties characteristic to the electrostatic and charge transfer processes. pKi is also influenced by steric properties characteristic to the unspecific interactions such as van der Waals and hydrogen bond interactions.

The results obtained should be related to the pharmacophore model proposed by Cook.[12] This pharmacophore contains three hydrophobic domains. In quinoxaline and quinazoline derivatives there are two regions defined by phenyl and *t*-Bu substituents on the saturate side of the 1,2,3,4-tetrahydroquinoxaline ring and another one on the opposite side, around the aromatic ring of quinoxaline. Also, the pharmacophore model contains three regions able to form hydrogen bonds, one can interact as donor and two regions as acceptors of hydrogen bonds.

## CONCLUSIONS

For a large set of quinoxaline and quinazoline derivatives active on the GABA/benzodiazepine receptor a classical QSAR study was performed using MTD and other descriptors calculated with DRAGON3.0 software.

MTD gives statistical significant but modest regression models with standard error of estimate around 0.5. Moreover, the MTD descriptor cannot be associated with other partner descriptors due to its high and complex information content.

The best regression model obtained contains ten descriptors that characterize the electrostatic and charge transfer interactions and also unspecific interactions such as hydrogen bond and van der Waals interactions.

The significance of the descriptors contained by the regression models suggests that the model is in accordance with the pharmacophore model proposed by Cook.

## REFERENCES


1. Jacobsen EJ, Stelzer LS, Belonga KL, Carter DB, Im WB, Sethy VH, Tang AH, Von Voigtlander PF, Petke JD, *J. Med. Chem*., **1996**, *39*, 3820.
2. TenBrink RE, Im WB, Sethy VH, Tang AH, Carter DB, *J. Med. Chem.*, **1994**, *37*, 758
3. Jacobsen EJ, Stelzer LS, TenBrink RE, Belonga KL, Carter DB, Im HK, Im WB, Sethy VH, Tang AH, Von Voigtlander PF, Petke JD, Zhong W-Z, Mickelson JW, *J. Med. Chem.*, **1999**, *42*, 1123.
4. Dewar MJS, Zoebisch EG, Healy EF, Stewart JJP, *J. Am. Chem. Soc.*, **1985**, *107*, 3902-3909.
5. HyperChem$^{(R)}$ release 7.52 for Windows, Hypercube, Inc. Gainsville, Florida, **2006**.
6. Simon Z, MTD and hyperstructure approaches. In *3D-QSAR in"Drug Design Theory, Methods, Applications"*, (H. Kubiny Ed.). ESCOM Leyden, **1993**, 307-319.
7. Simon Z, *Rev.Roum.Chim.*,**1987**, *32,* 1103.
8. Todeschini R, Consonni V, Mauri A, Pavan M, DRAGON 3.0, **2003**.
9. Parr RG, Pearson RG, *J. Am. Chem. Soc.*, **1983**, *105***,** 7512.
10. Pearson, RG, *Chemtracts-Inorg.Chem.*, **1991**, *3***,** 317.
11. StatSoft Inc., USA, STATISTICA for WINDOWS Release 5.0
12. Huang Q, He X, Ma C, Liu R, Yu S, Dayer CA, Wenger GR, McKernan R, Cook JM, *J .Med. Chem.*, **2000**, *43*, 71.

*Revue Roumaine de Chimie*, **2007**, *52*(8–9), 853–858

*Dedicated to Professor Victor-Emanuel Sahini on the occasion of his 80th anniversary*

# THE PRIVILEGED STRUCTURES HYPOTHESIS FOR G PROTEIN-COUPLED RECEPTORS – SOME PRELIMINARY RESULTS

Ramona RAD,[a] Maria MRACEC,[a*] Mircea MRACEC[a] and Tudor OPREA[b]

[a] Roumanian Academy, Institute of Chemistry Timisoara, 24 Mihai Viteazu Av., 300223-Roumania
[b] Division of Biocomputing, Department of Biochemistry and Molecular Biology, MSC11 6145, University of New Mexico School of Medicine, Albuquerque, NM 87131-0001, USA

*Received May 29, 2007*

Almost 20 years ago, the concept of privileged structures emerged as a potentially useful strategy in the discovery of novel biologically active compounds. Privileged structures are molecular fragments with versatile binding properties, i.e., structural chemotypes that are able to yield potent and often selective ligands for different biological targets through modification of functional groups. Thus, the identification of privileged structures becomes an important goal in the process of drug design. Herein we present a simple and efficient method for the identification of privileged structures targeting G-protein coupled receptor (GPCR).

## INTRODUCTION

Modern drug discovery is shifting focus from identifying suitable candidate drugs – which remains an essential but time-consuming goal – to identifying suitable candidate leads in order to maximize the cost-effectiveness and speed of the lead optimization process.[1–5] The industry is embarking in the process of efficient identification of small molecules, or small molecular fragments, which can further be optimized, in order to obtain lead structures. Though formulated almost two decades ago, the concept of privileged structures has received additional attention in recent years, in particular with the advent of combinatorial chemistry – where molecular libraries based on privileged structures are often given higher synthetic priority.

Briefly, this concept is based on the observation that certain chemical structural units occur in many ligands, *i.e.*, "privileged (sub)structures". Evans et al[6] noted that by chemical derivatization, such privileged structures can be used to develop new ligands. Often, privileged structures provide high-affinity ligands for more than one receptor subtype,[7] e.g., the benzodiazepine class of drugs. The privileged structure (or scaffold) concept has been successfully used in discovering novel ligands for e.g., new growth hormone secretagogue ligands were identified by screening privileged structure compounds from other receptors.[8,9] Yang et al.[10] reported the synthesis and characterization of L-054,522 a small peptidomimetic agonist with high potency and selectivity for somatostatin receptor subtype 2. This compound was synthesized using the privileged structure dipeptide strategy, the coupling of a dipeptide to a privileged structure.[11] This strategy was used with good results for the generation of active and selective ligands on the melanocortin subtype-4 receptor. [12–16]

G-protein coupled receptors (GPCRs) are one of the most therapeutically significant classes of drug targets, and the identification of (novel) privileged GPCR scaffolds remains a priority. We hypothesized that certain privileged structures – if confirmed – might have a higher propensity to occur in drugs that target GPCRs. Such an example is phenoxymethyl-ethanolamine, which one can historically trace back to epinephrine and nore

* Corresponding author: mracec@acad-icht.tm.edu.ro

pinephrine, the endogenous ligands that activate adrenergic receptors. Most of these structures act as antagonists on the adrenergic receptors (see Figure 1).

In this preliminary study, we examine the privileged structure hypothesis for GPCRs using a collection of literature compounds from the WOMBAT (World of Molecular BioAcTivity) database.[17] The choice for looking at GPCRs is related to the fact that at least 35% of the therapeutically important drug targets are members of the GPCR family.[18,19] We applied the MDL ISIS software[20] to generate substructures and to query for their presence in the WOMBAT database.[21] In this paper, we summarize results based on over 600 substructures, used to query the 2004.2 version of WOMBAT, then highlight substructures that appear to be more specific to GPCRs.

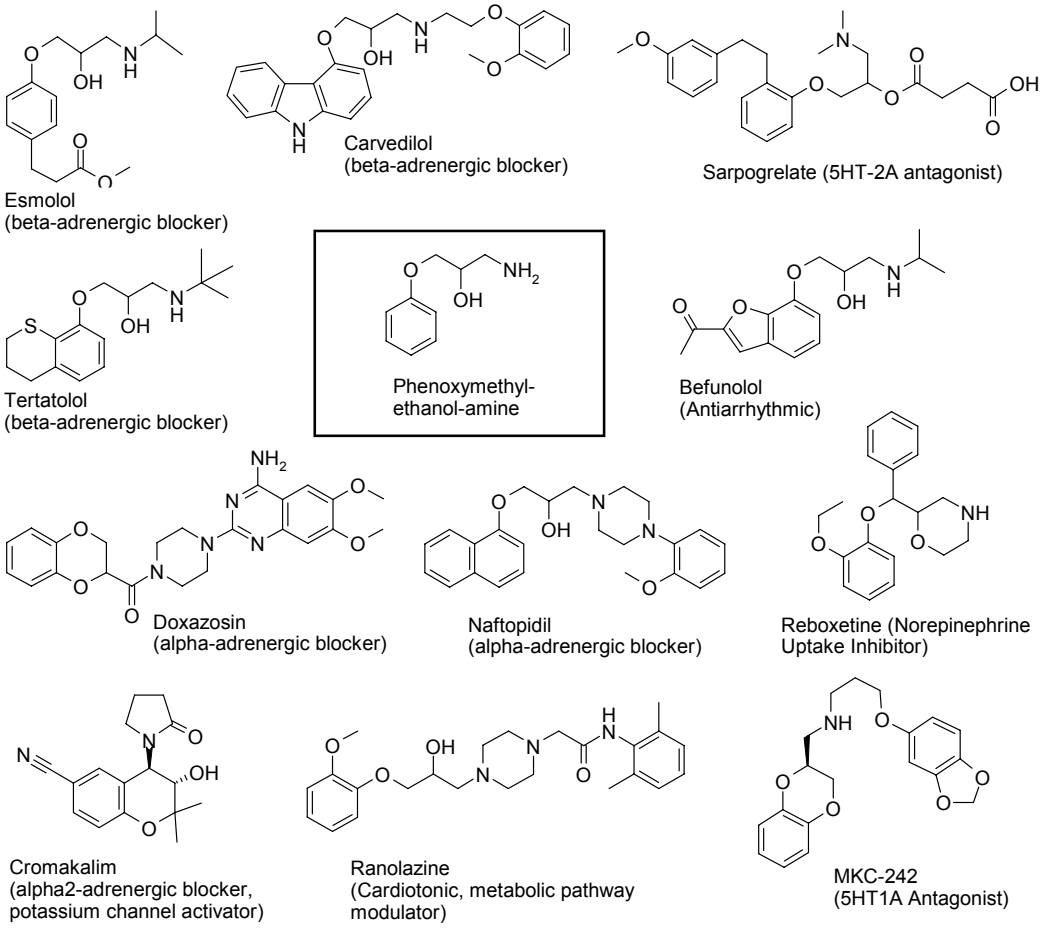


Fig. 1 – Drugs derived from phenoxymethyl-ethanolamine.
These structure were derived from norepinephrine, where catechol replaces the phenyl moiety.

## METHODS

All chemical structures were manually sketched in ISISDraw2.3.1, and used as query. We then used substructure searching (fragments) in ISIS/Base2.3.1, using the WOMBAT 2004.2 database. This database is a collection of structures gathered from recent Chemistry literature, for the most part, the Journal of Medicinal Chemistry (1991-2003), and contains over 80,000 entries. Of these, over 30,000 entries were ligands tested on GPCR targets. The vast majority of these ligands were tested *in vitro*, and approximately one third were tested on human (or recombinant human) GPCRs. Among the human-GPCR tested ligands, 1,230 have "generic names", i.e., they are in a higher development phase in the drug discovery process.

To further validate the substructures found in WOMBAT, we used the MDDR (MDL Drug Data Report) 2002 database, in particular the subset consisting of Phase I-III and Launched drugs. MDDR database is available from MDL.[22] We recorded the frequency of occurrences for each substructure, comparing WOMBAT-GPCR with

MDDR and MDDR-GPCR (where "GPCR" refers to GPCR-specific entries in the two databases). We considered the MDDR-GPCR subset to be "biologically validated", since compounds in Phase I or higher are already subject to intense scrutiny in terms of biological relevance for that particular GPCR target.

A number of 617 substructures were used for the query. Each substructure hypothesized to be privileged was stored separately in terms of occurrences in WOMBAT, in WOMBAT-GPCR, in MDDR and in MDDR-GPCR. Statistical processing of the results was performed in Microsoft Excel. For these 617 structures, the following notations were made: "F_GPCR" represents a fragment's occurrence in compounds from the WOMBAT-GPCR set, and "F_DIF" represents the difference between the number of compounds indexed in the entire WOMBAT database and the number of compounds from the WOMBAT-GPCR subset, which contain within their molecule the queried structure. The selection of chemically privileged fragments was performed based on the following selection criteria:

The first selection criterion: F_GPCR ≥ F_DIF,

The second criterion: F_GPCR > median. We calculated the median for F_GPCR values in order to eliminate those fragments which have a poor contribution to the signal/noise ratio

The third criterion: F_GPCR > enrichment factor (EF); where EF = 1- (F_DIF/F_GPCR). This criterion allows one to quickly highlight fragments that display a high frequency of occurrence.

## RESULTS AND DISCUSSION

Aimed at identifying privileged GPCR fragments, this preliminary study is focused on the hypothesis (are privileged substructure a valid concept?) and at cheminformatic tools that could formally be used to test this hypothesis. Several steps were observed:

Each fragment was queried separately on the two databases and their target subsets;

From these substructures, those that had relevant statistical values, i.e., F_GPCR occurrence above zero (F_GPCR >0) were considered for further study. Given this criterion, a number of 615 structures were maintained;

Criteria defined as above were applied to seek chemically privileged structures;

Biological validation of these "chemically privileged structures" was performed in MDDR.

First, we tested the: F_GPCR ≥ F_DIF condition. From 615 fragments with F_GPCR > 0, only 164 fragments met this criterion. These 154 structures were examined further; the F_GPCR median value was found to be set at 15. Therefore, the second selection criterion was set as F_GPCR >15. Out of 164 fragments, a subset of 82 (50%) had frequency higher than the median, which was not unexpected. These 82 structures underwent further filtering, in order to quantitatively assess the *enrichment* of a particular fragment relative to the GPCR target class.

The frequency occurrence of a specific fragment in the non-GPCR set (F_DIF) relative to its occurrence in the GPCR set was then used to determine the **enrichment factor, *EF.*** EF gives us a quantitative measure of the distribution of specific fragments in the GPCR subset relative to the entire database. EF values for each of the 82 significant substructures were calculated. We considered those fragments having EF values greater than the median of all EF values for the entire set of 82 fragments as "chemically privileged". While empirical, this criterion was used to improve the signal-noise ratio and to ascertain that only meaningful substructures were examined. As expected, 50% of these structures (41 fragments) met the final criterion, and we report these in Figure 2.

The concept of "biological validation" was introduced to further discriminate "chemically privileged" substructures (i.e., those that are recurring motifs in medicinal chemistry literature) from those privileged scaffolds that have indeed passed the test of biological and perhaps clinical significance, in a setting more relevant for drug discovery.

We used MDDR for this purpose, in particular its subset of compounds in Phase I (or higher) clinical testing, as well as the subset of marketed drugs. These compounds already comply with a minimum set of therapeutic requirements (including Safety), hence structures present in this subset are considered to be "biologically validated". After querying the 41 substructures in MDDR, the following observations were drawn. Only 6 fragments were biologically validated, namely F260, F457, F520, F543, F569, F596 in Figure 2 (these are labeled in **bold**). For some of these structures (F260, F520, F543) examples of drugs acting on GPCR which contain within their molecule the specified fragment (**in bold**) are displayed in Figure 3.

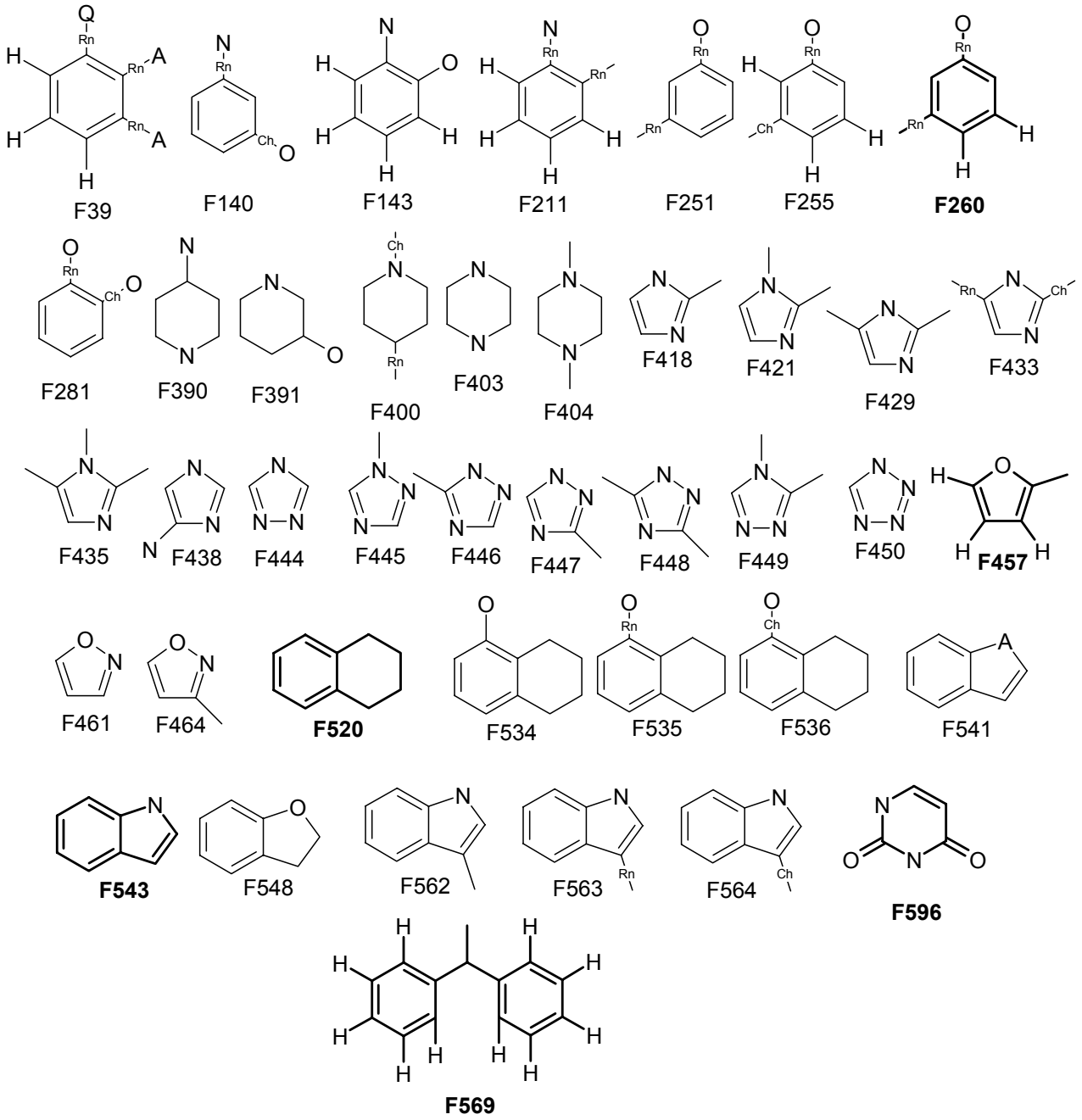


Fig. 2 – Chemically and biologically (bold) privileged structures.

Our preliminary results indicate that these 6 substructures are likely to be truly privileged scaffolds for GPCR targets. The remaining substructures remain, for now, "chemically privileged", since they are not present in this collection of clinically relevant structures. However, we do not exclude the possibility that some of them may, indeed, turn out to be "biologically privileged" as well, for two reasons: (i) this MDDR subset is not exhaustive; (ii) new drugs are approved every year, therefore this study provides only a snapshot relevant for the 2002 drugs.

## CONCLUSIONS

Our preliminary study illustrates the application of the privileged structure concept on a rather limited number of chemical structures, and further identifies 41 substructures that are "chemically privileged". Of these, only 6 appear to be biologically validated, which cautions one not to extending this concept onto a chemotype without first testing for clinical relevance. This study further suggests that the privileged substructure hypothesis is valid, at least with respect to those

substructures that pass the "biological validation" criterion. Mining databases of biologically compounds using simple cheminformatic tools can thus become useful in the process of guiding combinatory library synthesis, which could further yield potentially novel bioactive compounds for a specific category of biological targets.

*Acknowledgment:* Part of this work was supported by the NIH Molecular Libraries Initiative award U54 MH074425-01 (TIO).

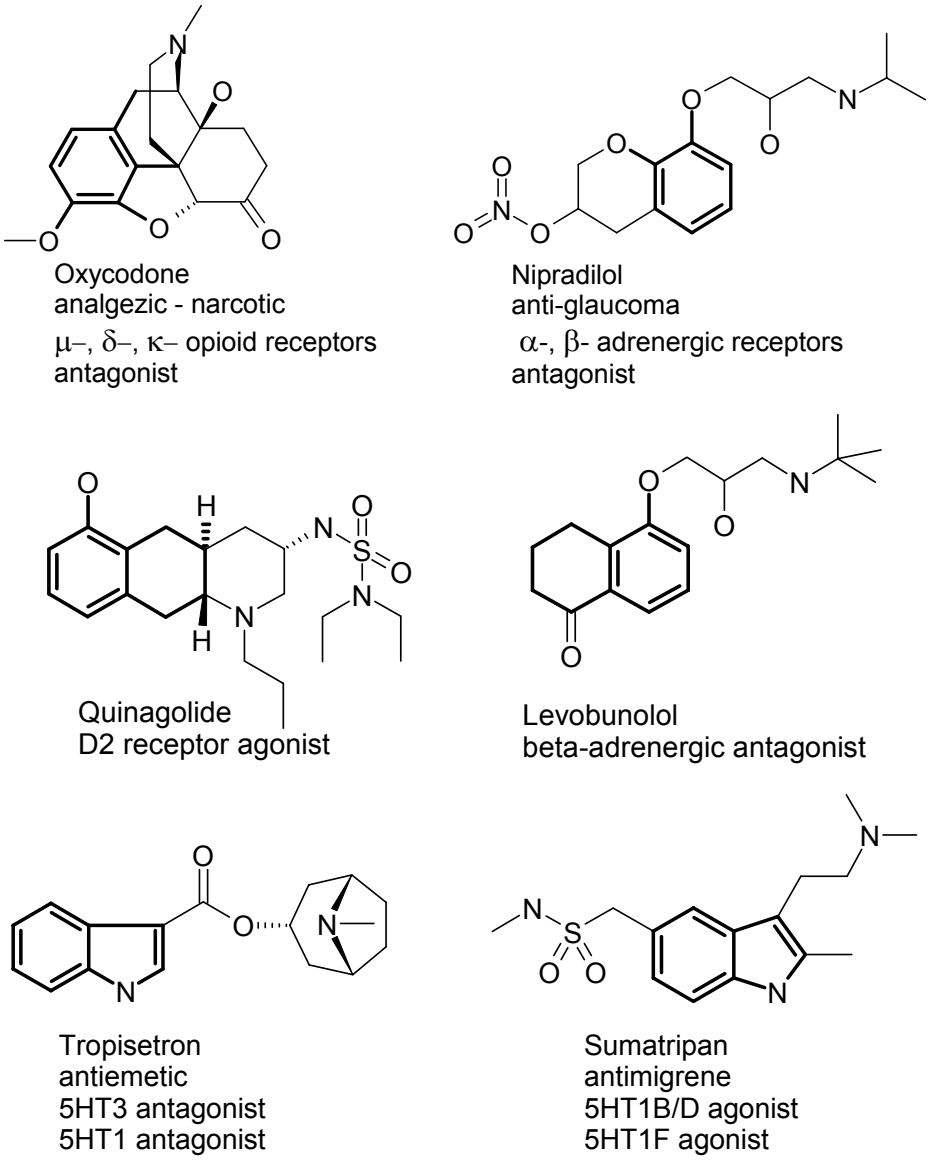


Fig. 3 – Examples of drugs acting on GPCR having in their molecules biologically (bold) privileged structures.

## REFERENCES

1. Oprea TI, *J. Comput.-Aided Mol. Des.* **2000**, *14*, 251-264.
2. Teague SJ, Davis AM, Leeson PD, Oprea TI, *Angew. Chem. Int. Edu.* **1999**, *38*, 3743-3748.
3. Oprea TI, Davis AM, Teague SJ, Leeson PD, *J. Chem. Inf. Comput. Sci.*, **2001**, *41*, 1308-1315.
4. Oprea TI, Gottfries J, *J. Comb. Chem,* **2001**, *3*, 157-166.
5. Nicolaou KC, Pfefferkorn JA, Roecker AJ, Cao G-Q, Barluenga S, Mitchell HJ, *J. Am. Chem. Soc.* **2000**, *122*, 9939-9953.
6. Evans BE, Rittle KE, Bock MG, DiPardo RM, Freidinger RM, Whitter WL, Lundell GF, Veber DF, Anderson PS, Chang RSL, Lotti VJ, Cerino DJ, Chen TB, Kling PJ, Kunkel KA, Springer JP, Hirshfield J, *J.Med.Chem* **1988**, *31*, 2235-2246
7. Horton DA, Bourne GT, Smythe ML, *Chem. Rev*. **2003**, *103*, 893-930
8. Patchett AA, Nargund RP, Tata JR, Chen M-H, Barakat KJ, Johnston DBR, Cheng K, Chan WW-S, Butler B, Hickey G, Jacks T, Scheim K, Pong S-S, Chaung L-YP, Chen H-Y, Fraizer E, Leung KH, Chiu S-HL, Smith RG, *Proc. Natl. Acad. Sci. USA* **1995**, *92*, 7001-7005.
9. Guo T, Hobbs DW, *Assay and Drug Development Technologies.* **2003**, *1*, 579-592.
10. Yang L, Berk SC, Rohrer SP, Mosley RT, Guo L, Underwood DJ, Arison BH, Birzin ET, Hayes EC, Mitra

SW, Parmar RM, Cheng K, Wu T-J, Butler BS, Foor F, Pasternak A, Pan Y, Silva M, Freidinger RM, Smith RG, Chapman K, Schaeffer JM, Patchett AA, *Proc. Natl. Acad. Sci. USA* **1998**, *95*, 10836-10841.
11. Nargund RP, Patchett AA, Bach MA, Murphy GM, Smith RG, *J.Med.Chem* **1998**, *41*, 2175-2179.
12. Sebhat IK, Martin WJ, Ye Z, Barakat K, Mosley RT, Johnston DBR, Bakshi R, Palucki B, Weinberg DH, MacNeil T, Kalyani RN, Tang R, Stearns RA, Miller RR, Tamvakopoulos C, Strack AM, McGowan E, Cashen DE, Drisko JE, Hom GJ, Howard AD, MacIntyre DE, van der Ploeg LHT, Patchett AA, Nargund RP, *J.Med.Chem.* **2002**, *45*, 4589-4593.
13. Pontillo J, Tran JA, Fleck BA, Marinkovic D, Arellano M, Tucci FC, Lanier M, Nelson J, Parker J, Saunders J, Murphy B, Foster AC, Chen C, *Bioorg. Med. Chem. Lett.* **2004**, *14*, 5605-5609.
14. Fischer MJ, Backer RT, Husain S, Hsiung HM, Mullaney JT, O'Brian TP, Ornstein PL, Rothaar RR, Zgombick JM, Briner K, *Bioorg. Med. Chem. Lett.* **2005**, *15*, 4459-4462.
15. Fischer MJ, Backer Collado I, de Frutos O, Husain S, Hsiung HM, Kuklish SL, Mateo AI, Mullaney JT, Ornstein PL, Garcia Paredes C, O'Brian TP, Richardson TI, Shah J, Zgombick JM, Briner K, *Bioorg. Med. Chem. Lett.* **2005**, *15*, 4973-4978.
16. Bakshi RK, Hong Q, Tang R, Kalyani RN, MacNeil T, Weinberg DH, van der Ploeg LHT, Patchett AA, Nargund RP, *Bioorg. Med. Chem. Lett.* **2006**, *16*, 1130-1133.
17. Olah M, Mracec M, Ostopovici L, Rad R, Bora A, Hadaruga N, Olah I, Banda M, Simon Z, Mracec M, Oprea TI, WOMBAT and WOMBAT-PK: Bioactivity Databases for Lead and Drug Discovery, in *Chemoinformatics in Drug Discovery.* T.I. Oprea (Ed), Wiley-VCH, NY, **2004**, 223-239.
18. Drews J, *Science* **2000**, *287*, 1960-1964
19. Overington JP, Al-Lazikani B, Hopkins AL, *Nature Rev.*, **2006**, *5*, 993-996.
20. ISISBase 2.1.3 software is available from MDL, http://mdli.com/
21. The WOMBAT database is available from http://www.sunsetmolecular.com/
22. The MDDR database is available from http://mdli.com/

*Revue Roumaine de Chimie*, **2007**, *52*(8–9), 859–867

*Dedicated to Professor Victor-Emanuel Sahini on the occasion of his 80th anniversary*

# AM1 CONFORMATIONAL ANALYSIS OF THE (3S,5R,6R)-6-ACETYLAMIDOPENICILLANIC ACID

Mihaela SCHULTZ, Maria MRACEC, Eugen SISU and Mircea MRACEC*

Roumanian Academy, Institute of Chemistry Timisoara , Bd. Mihai Viteazul 24, RO-300223 Timisoara, ROUMANIA, e-mail: mracec@acad-icht.tm.edu.ro

*Received March 6, 2007*

Using the AM1 semiempirical MO method a conformational search study was performed for the conformers of the (3S,5R,6R)-6-acetylamidopenicillanic acid. The AM1 method gives 8 distinct conformers. The difference between the heat of formation of the minimum energy conformer and the one of the highest energy conformer is of 7.12 kcal/mol. The AM1 calculated bond lengths and angles for the minimum energy conformer are close to the experimentally determined values. The steric and electronic properties of the AM1 conformers are influenced by the orientation of the substituent attached to the amidic group bound at the lactamic ring.

## INTRODUCTION

The (3S,5R,6R)-6-acetylamidopenicillanic acid is one of the most known antibacterials of the penicillin class. As all penicillins, its molecular structure contains two fused rings (a β-lactamic four-membered ring and a thiazolidinic five-membered ring) having three chiral centers[1] noted with an asterisk in Fig. 1. Due to these chiral centers there are $2^3$=8 possible diastereoisomers: 3R,5R,6R; 3S,5R,6R; 3R,5S,6R; 3R,5R,6S; 3S,5S,6R; 3S,5R,6S; 3R,5S,6S; 3S,5S,6S.[2] The 3S,5R,6R diastereoisomer is the natural product. Its two-fused rings represent the general structure of all antibacterials of the penicillin class.[3] Among the hypotheses on the action mechanism of penicillins the experimental data confirmed Strominger's hypothesis. He demonstrated that the D-Ala-D-Ala sequence from the general structure of penicillins is responsible for their antibacterial activity.[3-7] The thick line in Fig. 1 shows the key atoms forming the D-Ala-D-Ala sequence of the penicillin backbone.[8] The molecular and electronic structures of the (3S,5R,6R)-natural isomers of penicillins have been extensively studied with different quantum-chemical methods.[9-15] All used quantum-chemical methods give a pyramidalized structure for the amidic nitrogen atoms, but in none of these works is mentioned the degree of pyramidalization of the N14 amidic nitrogen atom. This effect influences the results of the quantumchemical methods applied to structures with rotatable bonds.[16]

The present study analyzes the possibility to obtain a maximum number of distinct conformers of the (3S,5R,6R)-6-acetylamidopenicillanic acid by performing a conformational search using the AM1 semiempirical MO method. The influence of the substituents on the molecular and electronic structure of these conformers is also analyzed.

## METHODS

The gas phase equilibrium geometry of the conformers was obtained by AM1 calculations with an SCF convergence of $10^{-5}$ and a RMS gradient of $10^{-2}$ kcal/Å·mol. Conformational search was performed by varying the C2-C3-C11-C12, C5-C6-N14-C15 and C6-N14-C15-C16 dihedrals in the range 0 ±180° with steps of 15°. The energy criterion was set to 30 kcal/mol above the minimum energy conformer. The calculations have been performed with the Conformational Search module

from the HyperChem7.52 package.[17] In order to obtain all conformers, including the minimum energy conformer, for structures with more than two flexible bonds the conformational search is generally performed by the grid method.[16-18] For around 99% of the possible conformers we should know approximately the minimum ratio between the number of starting grid points and the number of possible conformers. To find this ratio a plot of the dependence of number of conformers on the number of starting grid points is presented in Fig. 2.

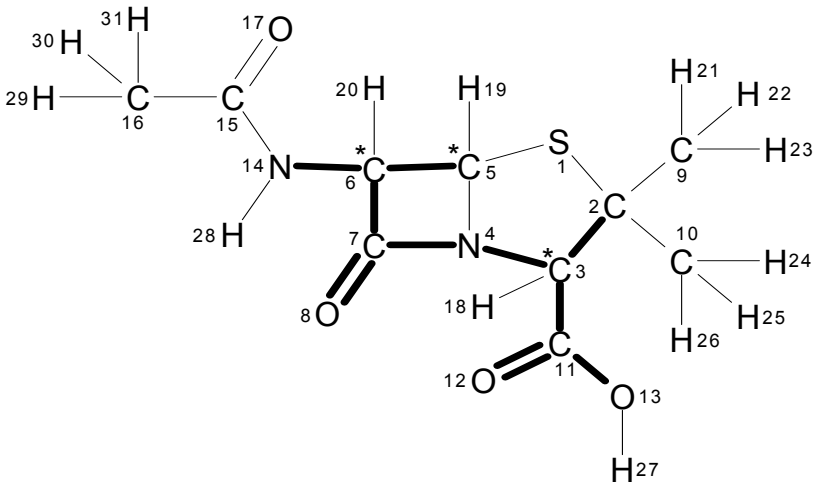


Fig. 1 – Atom numbering of the (3S,5R,6R)-6-acetylamidopenicillanic acid (the three chiral centres: C3, C5 and C6 are marked with asterisks).

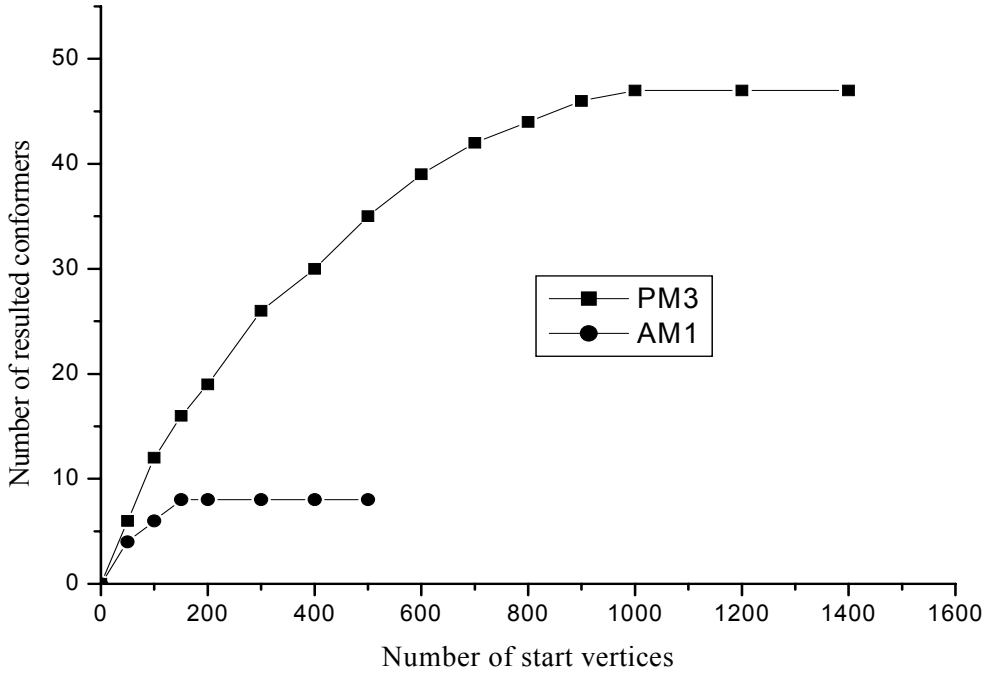


Fig. 2 – Functional dependence of the number of discovered conformers based on the number of starting geometries for the AM1 and PM3 semiempirical MO methods.

Fig 2 shows that for the PM3 method only after around 1000 starting geometries the total number of 47 distinct conformers remains constant, while for the AM1 method the total number of 8 distinct conformers remains constant after 150 starting geometries. This data leads to the conclusion that for obtaining the maximum number of possible conformers the ratio between the number of starting points and the number of possible conformers should be around 20:1.

## RESULTS

The AM1 method gives structures with pyramidalized nitrogen atoms and consequently generates a pseudochiral configuration for the N14 atom in the penicillanic acid.[19] The C6-C15-H28-N14 improper dihedral was used to measure "conicity" of the out-of-plane substituents at the N14 nitrogen atom. This "conicity" could be considered a measure of the degree of pyramidalization of the N14 atom. For a planar structure of the substituents around the N14 atom, this dihedral is 0°. The amidic groups can have *anti* or *syn* relative positions of the O17 and H28 atoms. For all resulted conformers the AM1 method gives lower energy for structures with *anti* amidic groups than the energy of those with *syn* amidic groups. To be sure that the obtained conformers are minima on the potential energy surface and not saddle points, for each conformer was performed a calculation of normal vibrations. All vibrations are positive, including $\nu_{min}>0$. The wavelength number of the maximum vibration, $\nu_{MAX}$ and zero point vibrational energy (ZPVE) are given in Table 1.

The geometric and electronic data of the conformers resulted from conformational search are displayed in Tables 1-6. The total energy, $E_{tot}$, was used to order the conformers. To analyze the results given by the AM1 method, the geometry of conformers was compared with the X-ray structure[20] of the (2S,5R,6R)-3,3-dimethyl-7-oxo-6-phenylacetylamino-4-thia-1-aza-bicyclo

[3.2.0]heptane-2-carboxylic acid 1-ethoxycarbonyloxy-ethyl ester by measuring the ring and the exocyclic bond lengths, the ring bond angles including those that measure the bending of the two fused rings, and some proper and improper dihedrals. By selecting the atoms in the same order in the X-ray geometry and in the geometry of each conformer, the structures have been superposed and the RMS fit errors were calculated.

The AM1 method gives 8 distinct conformers (Tab. 1). Between the heat of formation of the minimum energy conformer (1am1) and the heat of formation of the conformer with the highest energy (8am1) is a difference of 7.12 kcal/mol.

*Table 1*

Some structural and energetic characteristics of the conformers resulted from AM1 calculations for the (3S,5R,6R)-6-acetilamidopenicilanic acid, arranged according to the decreasing variation of the total calculated energy and heat of formation, compared to some experimental data

| **Enegetic order** | **$E_{tot}$** (kcal/mol) | **$\Delta H_{form}$** (kcal/mol) | **$IP_1$** (eV) | **$EA_1$** (eV) | ***μ*** (Debye) | Dihedral angles (°) | | Improper angle (°) | **Chirality** N14 | **Position** O17, H28 |
|---|---|---|---|---|---|---|---|---|---|---|
| | | | | | | **5-1-2-3** | **5-2-3-4** | **6-15-28-14** | | |
| 1am1 | -77547.31 | -122.404 | -9.350 | -0.042 | 5.203 | 5.688 | 18.157 | -8.460 | R | Anti |
| 2am1 | -77546.94 | -122.037 | -9.369 | -0.052 | 4.704 | 5.211 | 17.922 | -8.348 | R | Anti |
| 3am1 | -77546.22 | -121.316 | -9.371 | -0.100 | 1.779 | 7.073 | 18.065 | -1.067 | - | Syn |
| 4am1 | -77545.77 | -120.871 | -9.392 | -0.112 | 2.563 | 6.596 | 17.651 | -0.658 | - | Syn |
| 5am1 | -77543.51 | -118.604 | -8.978 | 0.282 | 4.410 | -1.606 | 8.824 | 7.579 | S | Anti |
| 6am1 | -77543.06 | -118.154 | -8.994 | 0.274 | 5.632 | -1.877 | 8.298 | 7.563 | S | Anti |
| 7am1 | -77540.57 | -115.667 | -9.269 | -0.091 | 2.434 | -12.53 | 4.173 | 7.496 | S | Syn |
| 8am1 | -77540.19 | -115.284 | -9.283 | -0.102 | 2.776 | -12.59 | 3.926 | 7.512 | S | Syn |
| Expr.**Data**[20] | - | - | - | - | - | 17.583 | 40.263 | -1.145 | - | Anti |
| Expr.**AMPC**[21] | - | - | - | - | - | 40.3 | -9.7 | - | - | - |
| Expr.**PN09**[21] | - | - | - | - | - | 21.1 | -144.6 | - | - | - |
| Expr.**PN14**[21] | - | - | - | - | - | -40.9 | -2.9 | - | - | - |
| Expr.**PN39**[21] | - | - | - | - | - | 16.9 | 36.6 | - | - | - |

The first four conformers in Table 1 have negative conicity and (R)-pseudochirality at the N14 atom, while the last four conformers have positive conicity and (S)-pseudochirality at the N14 atom. In the minimum energy conformer the amidic group atoms have *anti* orientation, while in the highest energy conformer the amidic atoms have *syn* orientation. First two conformers have a pronounced negative conicity at the N14 atom (around -8.5º), while the following two conformers have a conicity at the N14 atom near 0º. In these conformers the amidic group is almost planar. Although the conformers 3am1 and 4am1 have around N14 a "conicity" near 0º the atoms of this amido group have a *syn* orientation and therefore a lower steric likeness (0.932Å respectively 1.179Å) comparing to the experimental geometry. The last four conformers have a conicity around 7.5º. Energy differences of 1.088, 1.166, 2.937, and 2.870 kcal/mol resulted between the pairs of conformers 1am1→3am1, 2am1→4am1, 5am1→7am1 and 6am1→8am1 having the amidic bonds in *anti* and *syn* respectively. The energy difference between the two orientations of the carboxylic function is of 0.367 kcal/mol for the first two conformers and of 0.450 kcal/mol for the 5am1 and 6am1 conformers.

The superimposition of all conformers using the plane formed by the N4, C5 and C6 atoms is given in Fig. 3. According to this superimposition, the conformers can be classified in three groups with different puckering of the thiazolidinic ring: *i*) 1am - 4am1, *ii*) 5am1 - 6am1, and *iii*) 7am1 - 8am1. The data in Tab. 1 shows that the first four conformers have a positive puckering given by the 5-1-2-3 dihedral (5.21º for conformer 2am1 and 7.07º for conformer 3am1), and by the 5-2-3-4 dihedral (17.65º for conformer 4am1 and 18.16º for conformer 1am1). The second group of conformers (5am1 and 6am1) have a negative puckering almost close to zero for the 5-1-2-3 dihedral and around -8.5º for the 5-2-3-4 dihedral. The last two conformers have an accentuated negative puckering of -12.5º for the 5-1-2-3 dihedral and around -4º for the 5-2-3-4 dihedral. The puckering is not generated by the rotation of the carboxylic group, but by the rotation around the C5-N14 and N14-C15 bonds. All the types of puckering are evidenced in Fig. 3. It should also be mentioned that in the experimentally determined structure[21] the thiazolidinic ring is also puckered.

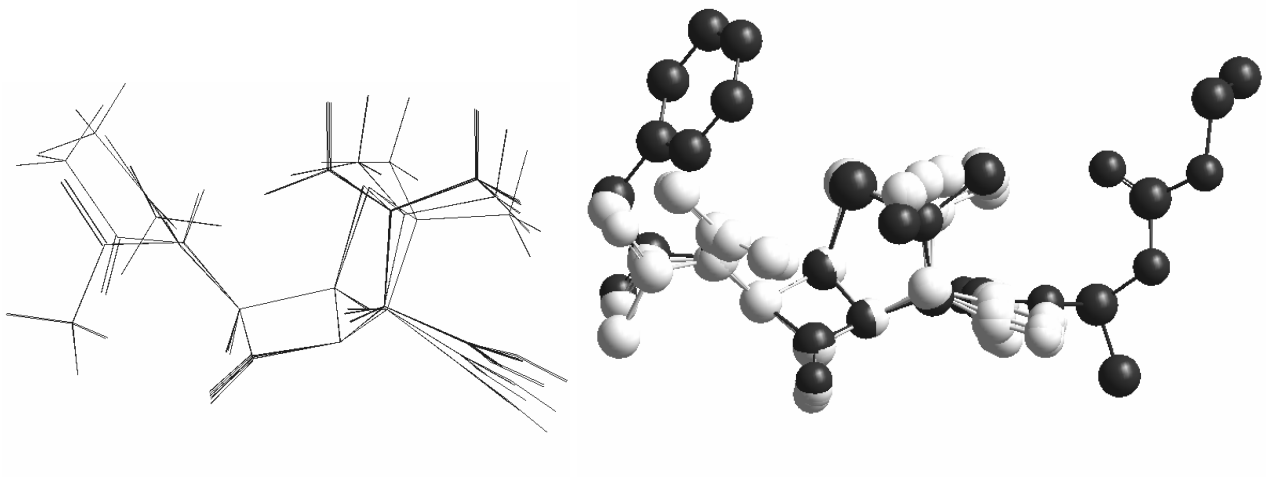

(a) (b)

Fig. 3 – Superimposition of all AM1 conformers (a) and superimposition of the heavy atoms in the experimental geometry (black atoms),[21] over the heavy atoms of the 8 AM1 conformers (b).

There is no correlation between the energy or geometric data of the conformers and the ionization energies or the electron affinities (Tab. 1.). One can observe only that their values are ordered in *anti* - *syn* pairs of conformers.

For all the AM1 conformers both the highest occupied molecular orbital (HOMO = - $IE_1$) as well as the lowest unoccupied molecular orbital (LUMO = - $EA_1$) are dominated by the contribution of the sulfur atom S1 (Fig. 4). At the HOMO level, beside the sulfur atom, the C5-C6, C5-H19 and C2-C9, C2-C10 σ bonds have also an important contribution, while at the LUMO level the contribution of the C2 respectively C5 atoms are important. For the dipole moments the *syn* structures have values sensibly lower than the *anti* structures (Tab. 1.)

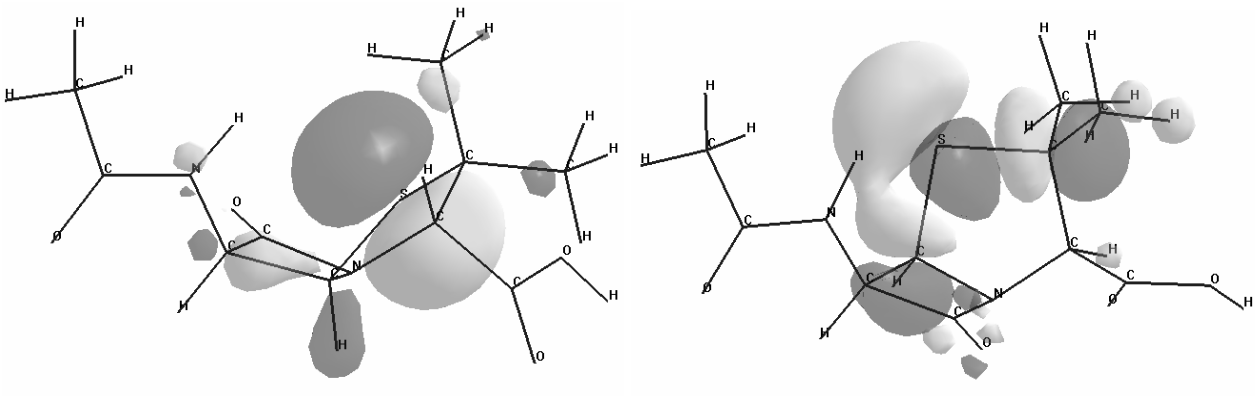

$-IP_1$ = HOMO $-EA_1$ = LUMO

Fig. 4 – Sulfur atom predomination both in the HOMO ($IP_1$) as well as in the LUMO ($EA_1$).

The net charge on the sulfur S1 atom is slightly positive, while the net charges on the N4, N14, O8, O12, O13, O17 atoms are negative in all conformers (Tab. 2.). Although the two nitrogen atoms (N4, N14) are of the same type, namely amidic atoms, the N4 atom is the strongest pyramidalized due to its position between the two fused rings. It has, as expected, a net charge lower than that of the N14 exocylic nitrogen atom. The net charge of the β-lactamic oxygen atom (O8) is lower than the net charges of the other oxygen atoms (O12, O13, O17). There are no evident correlations between net atomic charges and energy or geometric data of the AM1 conformers.

The electrostatic potential isosurface for the lowest and highest energy conformers (1am1) and (8am1) respectively are shown in Fig. 5. As can be seen in Fig 5 the shapes of the isosurfaces are influenced mainly by the rotation of the exocyclic amidic bond.

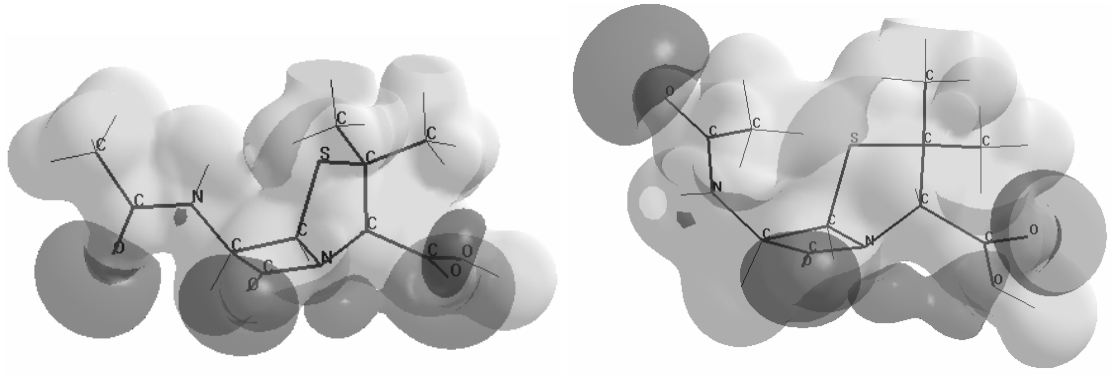

1am1 8am1

Fig. 5 – Electrostatic potential isosurfaces calculated with the AM1 method.

*Table 2*

Charge densities on some representative atoms, extreme vibration frequencies ($\nu_{min.}$, $\nu_{MAX.}$) and the vibration energy for the equilibrium state of the conformers resulted from AM1 computation, for the (3S,5R,6R)-6-acetilamidopenicilanic acid, arranged according to the decreasing variation of the calculated heat of formation

| Enegy order | $\Delta H_{form}$ (kcal/mol) | Net charge on atom | | | | | | | Vibration ($cm^{-1}$) | | ZPVE (kcal/mol) |
|---|---|---|---|---|---|---|---|---|---|---|---|
| | | S1 | N4 | N14 | O8 | O12 | O13 | O17 | $\nu_{min.}$ | $\nu_{MAX.}$ | |
| 1am1 | -122.404 | 0.043 | -0.258 | -0.370 | -0.239 | -0.331 | -0.310 | -0.348 | 31.18 | 3439.91 | 154.299 |
| 2am1 | -122.037 | 0.041 | -0.258 | -0.370 | -0.238 | -0.356 | -0.292 | -0.348 | 31.91 | 3440.34 | 154.325 |
| 3am1 | -121.316 | 0.069 | -0.256 | -0.379 | -0.242 | -0.332 | -0.318 | -0.346 | 23.03 | 3422.70 | 154.440 |
| 4am1 | -120.871 | 0.067 | -0.256 | -0.380 | -0.241 | -0.354 | -0.293 | -0.345 | 22.78 | 3413.17 | 154.464 |
| 5am1 | -118.604 | 0.050 | -0.260 | -0.362 | -0.229 | -0.339 | -0.318 | -0.360 | 27.94 | 3481.12 | 154.529 |
| 6am1 | -118.154 | 0.049 | -0.259 | -0.362 | -0.228 | -0.359 | -0.294 | -0.359 | 27.22 | 3481.59 | 154.562 |
| 7am1 | -115.607 | 0.074 | -0.263 | -0.367 | -0.248 | -0.330 | -0.318 | -0.348 | 27.74 | 3426.53 | 154.734 |
| 8am1 | -115.284 | 0.076 | -0.262 | -0.367 | -0.247 | -0.355 | -0.290 | -0.348 | 27.79 | 3426.68 | 154.777 |

In Fig. 6 it can be observed that the fundamental vibration $\nu_{min.}$ is a backbone vibration where all atoms are implicated. The movement vectors are proportional with the AM1 calculated force constants. The maximum energy vibration $\nu_{MAX}$ is an elongation vibration of the N14 - H28 bond. For all AM1 conformers the nature of these two vibrations does not change. The equilibrium zero point energy (ZPVE) is relatively constant around the value of 154.5 kcal/mol. It increases insignificantly from around 154.299 kcal/mol for the minimum energy conformer to 154.777 kcal/mol for the conformer of maximum energy. In a *syn* – *anti* pair of conformers the energy difference between a structure with an *anti* amidic group and a structure with a *syn* amidic group is of 0.1 kcal/mol.

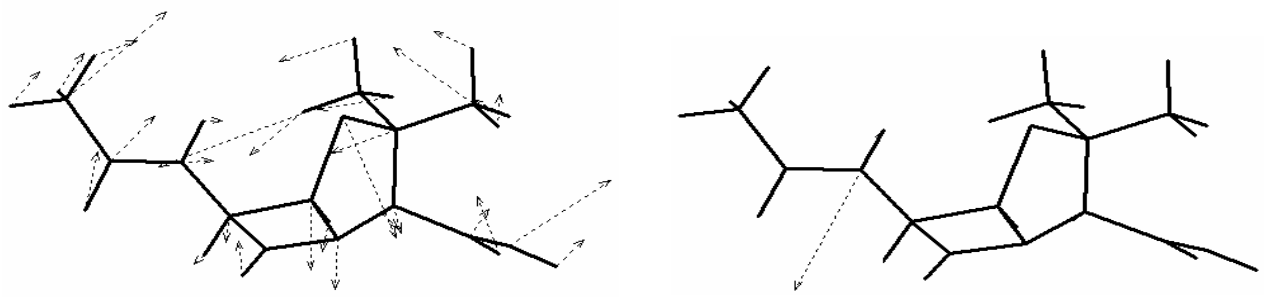

Fig. 6 – Movement vectors resulted from AM1 calculations for vibrations $\nu_{min} = 31.18$ cm$^{-1}$ and $\nu_{MAX} = 3439.91$ cm$^{-1}$ of the conformer 1am1.

A relatively good likeness (RMS error = 0.356Å) between the AM1 minimum energy conformer and the experimental geometry,[3,20,21] resulted from the comparison of the calculated and experimental values of bond lengths (Tables 3 and 4). Regarding the values calculated with semiempirical methods,[9] for other models of penicillins the differences resulted from the AM1 and PM3 semiempirical MO methods are of the same order, while the ab initio and DFT methods[10] give values much closer to the experimentally determined values (Tab. 3 and 4). The values of the S1-C2 bond lengths obtained in this paper are around 1.82Å, slightly higher than the S1-C5 bond lengths which are aproximately 1.78Å. This difference between the above two bond lengths is also observed experimentally. Curiously, the advanced methods HF/6-31G* and B3LYP/6-31G**,[10] do not reproduce this difference (Tab. 3 and 4).

The C2-C3, C3-N4, and N4-C5 bond lengths for all AM1 conformers are comparable with the experimentally obtained values and in a good concordance with the advanced HF/6-31G* and B3LYP/6-31G** methods. For the bonds in the β-lactamic ring: C5-C6, C6-C7 and N4-C7, the calculated values are slightly greater than the experimentally obtained values. For distances between the S1 and C9 ($C_\alpha$), respectively S1 and C10 ($C_\beta$) unbound atoms the calculated values are slightly lower than those experimentally obtained.[20] From the values in Table 3 and 4 one can conclude that the geometry of the AM1 conformers is strongly influenced by the exocyclic function bound through the amidic group to the C6 atom. Actually, this function is the one that also determines the variation of the biological activity of the different penicillines.

The calculated bond angles of the cycles and the 4-5-6-7 improper angle which measures the planarity of the β-lactamic cycle compared to the experimentally obtained values,[3,20,21] or obtained by other authors,[9,10] are presented in Tab. 5 and 6.

The AM1 values for the 4-5-6-7 improper angle indicate that the β-lactamic cycle for all conformers is not plane, but has a slight positive puckering. This positive puckering can also be observed in experimental data. A grouping in pairs *anti-syn* can also be observed, which suggests that the rotation of the carboxylic group with 180º does not influence significantly the puckering of the β-lactamic ring. Puckering of the β-lactamic cycle could be rather influenced by the conformation of the substituent attached to the C6 atom. The values for the 2-1-5, 5-4-7, 4-5-6, 5-6-7, 6-7-4 angles are in the range of the experimentally obtained values, while the 1-2-3, 2-3-4 and 1-5-4 angles are greater than the experimental values, and the angle 3-4-5 is lower than the experimental value. The bending angles between the thiazolidinic and β-lactamic rings split the conformers into two distinctive groups: the (R) conformers (Tab. 5) and the (S) conformers (Tab. 6). The 1-5-6 bending angle for the (R) conformers is close to the experimental value, while for the (S) conformers the values are lower than the experimental ones. The 3-4-7 bending angle is greater than the experimental value both for the (R) as well as for the (S) conformers.

*Table 3*

Bond lengths of the cycles and the exocyclic distances from the sulphur atom of the metil groups for the conformers resulted from AM1 calculations, for the (3S,5R,6R)-6-acetilamidopenicilanic acid, with R pseudochirality at the N14 nitrogen atom, arranged according to the decreasing variation of the calculated heat of formation, compared to some experimental and computed data in literature

| **Enegetic order** | **$\Delta H_{form}$ (kcal/mol)** | **Bond lengths (Å)** | | | | | | | | **Distance (Å)** | | **RMS Fit** |
|---|---|---|---|---|---|---|---|---|---|---|---|---|
| | | **S1-C2** | **C2-C3** | **C3-N4** | **N4-C5** | **C5-S1** | **C5-C6** | **C6-C7** | **C7-N4** | **S1-C9** | **S1-C10** | **RMS Error(Å)** |
| 1am1 | -122.404 | 1.821 | 1.560 | 1.446 | 1.477 | 1.785 | 1.582 | 1.568 | 1.447 | 2.710 | 2.700 | 0.356 |
| 2am1 | -122.037 | 1.821 | 1.560 | 1.445 | 1.477 | 1.785 | 1.582 | 1.568 | 1.447 | 2.710 | 2.699 | 0.811 |
| 3am1 | -121.316 | 1.820 | 1.560 | 1.447 | 1.479 | 1.781 | 1.582 | 1.572 | 1.444 | 2.712 | 2.698 | 0.932 |
| 4am1 | -120.871 | 1.821 | 1.560 | 1.446 | 1.479 | 1.781 | 1.582 | 1.572 | 1.444 | 2.711 | 2.697 | 1.179 |
| Exp.**Data**[20] | - | *1.860* | *1.573* | *1.458* | *1.465* | *1.824* | *1.550* | *1.547* | *1.376* | *2.779* | *2.749* | - |
| Exp.**AMPC**[21] | - | *1.854* | *1.556* | *1.466* | *1.466* | *1.812* | *1.528* | *1.528* | *1.382* | - | - | - |
| Exp.**AMPC**[3] | - | *1.855* | *1.573* | *1.463* | *1.470* | *1.791* | *1.554* | *1.540* | *1.360* | - | - | - |
| Exp.**PN09**[21] | - | *1.859* | *1.564* | *1.468* | *1.476* | *1.815* | *1.561* | *1.541* | *1.367* | - | - | - |
| Exp.**PN14**[21] | - | *1.841* | *1.554* | *1.449* | *1.486* | *1.835* | *1.551* | *1.536* | *1.389* | - | - | - |
| Exp.**PN39**[21] | - | *1.857* | *1.567* | *1.450* | *1.457* | *1.838* | *1.546* | *1.542* | *1.378* | - | - | - |
| Exp.**PenV**[3] | - | *1.87* | *1.57* | *1.46* | *1.52* | *1.82* | *1.58* | *1.55* | *1.46* | - | - | - |
| Exp.**6APA**[3,21] | - | *1.859* | *1.575* | *1.445* | *1.450* | *1.822* | *1.554* | *1.520* | *1.392* | - | - | - |
| (ax.) HF/6-31G*[10] | - | 1.831 | 1.539 | 1.446 | 1.456 | 1.835 | 1.546 | 1.526 | 1.388 | - | - | - |
| (eq.) HF/6-31G*[10] | - | 1.825 | 1.546 | 1.452 | 1.457 | 1.823 | 1.544 | 1.527 | 1.383 | - | - | - |
| (ax.) B3LYP/6-31G**[10] | - | 1.851 | 1.545 | 1.454 | 1.470 | 1.863 | 1.554 | 1.542 | 1.407 | - | - | - |
| (eq.) B3LYP/6-31G**[10] | - | 1.846 | 1.552 | 1.460 | 1.469 | 1.850 | 1.551 | 1.543 | 1.402 | - | - | - |
| AM1[9] | - | 1.821 | - | - | - | 1.786 | - | - | 1.447 | - | - | - |
| PM3[9] | - | 1.875 | - | - | - | 1.815 | - | - | 1.481 | - | - | - |

*Table 4*

Bond lengths of the cycles and the exocyclic distances from the sulphur atom of the metil groups for the conformers resulted from AM1 calculations, for the (3S,5R,6R)-6-acetilamidopenicilanic acid, with S pseudochirality at the N14 nitrogen atom, arranged according to the decreasing variation of the calculated heat of formation, compared to some experimental and computed data in literature

| **Enegetic order** | **$\Delta H_{form}$ (kcal/mol)** | **Bond lengths (Å)** | | | | | | | | **Distances (Å)** | | **RMS Fit** |
|---|---|---|---|---|---|---|---|---|---|---|---|---|
| | | **S1-C2** | **C2-C3** | **C3-N4** | **N4-C5** | **C5-S1** | **C5-C6** | **C6-C7** | **C7-N4** | **S1-C9** | **S1-C10** | **RMS Error(Å)** |
| 5am1 | -118.604 | 1.8240 | 1.5607 | 1.4466 | 1.4770 | 1.7759 | 1.5868 | 1.5651 | 1.4437 | 2.7163 | 2.6902 | 1.145 |
| 6am1 | -118.154 | 1.8243 | 1.5609 | 1.4460 | 1.4772 | 1.7749 | 1.5869 | 1.5650 | 1.4438 | 2.7157 | 2.6894 | 1.330 |
| 7am1 | -115.667 | 1.8211 | 1.5611 | 1.4470 | 1.4772 | 1.7777 | 1.5893 | 1.5631 | 1.4396 | 2.7073 | 2.6983 | 1.203 |
| 8am1 | -115.284 | 1.8214 | 1.5614 | 1.4462 | 1.4774 | 1.7771 | 1.5893 | 1.5629 | 1.4399 | 2.7070 | 2.6975 | 1.374 |

*Table 5*

Bond angles of the cycles and the dihedral improper angle for the β-lactamic cycle of the conformers resulted from AM1 calculations for the (3S,5R,6R)-6-acetilamidopenicilanic acid with R pseudochirality at the N14 nitrogen atom, arranged according to the decreasing variation of the heat of formation, compared to some experimental and computed data in literature

| **Enegetic order** | **Angle (°)** | | | | | | | | | | | **Dihedral (°)** |
|---|---|---|---|---|---|---|---|---|---|---|---|---|
| | **C2-S1-C5** | **S1-C2-C3** | **C2-C3-N4** | **C3-N4-C5** | **S1-C5-N4** | **C5-N4-C7** | **N4-C5-C6** | **C5-C6-C7** | **C6-C7-N4** | **S1-C5-C6** | **C3-N4-C7** | **N4-C5-C6-C7** |
| 1am1 | 95.124 | 106.964 | 111.280 | 114.380 | 109.624 | 93.343 | 89.691 | 84.963 | 91.320 | 118.315 | 121.688 | 5.967 |
| 2am1 | 95.103 | 107.007 | 111.270 | 114.458 | 109.610 | 93.328 | 89.698 | 84.955 | 91.324 | 118.300 | 121.730 | 6.012 |
| 3am1 | 95.097 | 106.950 | 111.193 | 114.263 | 109.831 | 93.448 | 89.736 | 84.860 | 91.411 | 118.806 | 121.814 | 5.315 |
| 4am1 | 95.090 | 107.000 | 111.199 | 114.357 | 109.827 | 93.421 | 89.755 | 84.854 | 91.430 | 118.800 | 121.783 | 5.294 |
| Expr.**Data**[20] | *95.190* | *104.168* | *105.893* | *116.134* | *105.264* | *94.396* | *88.129* | *84.692* | *91.541* | *118.203* | *127.633* | *7.818* |
| Expr.**AMPC**[21] | *90.4* | *103.1* | *106.0* | *117.9* | *103.8* | *93.7* | *88.5* | *85.7* | *91.6* | *118.9* | *126.1* | *4.3* |
| Expr.**AMPC**[3] | *89.8* | *104.2* | *105.3* | *117.8* | *103.4* | *93.4* | *88.4* | *83.6* | *93.1* | *118.4* | *127.7* | - |
| Expr.**PN09**[21] | *95.2* | *103.9* | *105.6* | *115.8* | *105.5* | *94.2* | *87.7* | *84.4* | *92.6* | *118.9* | *126.7* | *7.1* |
| Expr.**PN14**[21] | *89.6* | *103.2* | *107.4* | *115.9* | *103.1* | *92.2* | *87.6* | *84.4* | *91.8* | *117.0* | *123.3* | *14.0* |
| Expr.**PN39**[21] | *94.9* | *105.0* | *106.0* | *117.2* | *105.8* | *93.8* | *88.8* | *84.2* | *92.0* | *119.3* | *126.7* | *7.0* |
| Expr.**PenV**[3] | *96.0* | *105.0* | *104.0* | *120.0* | *103.0* | *88.0* | *92.0* | *83.0* | *96.0* | *122.0* | *129.0* | - |
| Expr.**6APA**[3,21] | *95.6* | *105.7* | *106.0* | *118.0* | *103.7* | *93.5* | *88.1* | *84.6* | *91.7* | *120.2* | *132.5* | - |
| (ax.) HF/6-31G*[10] | 93.3 | - | - | 116.1 | - | - | 88.8 | - | - | 119.0 | - | - |
| (eq.) HF/6-31G*[10] | 90.2 | - | - | 117.8 | - | - | 88.8 | - | - | 117.4 | - | - |
| (ax.) B3LYP/6-31G**[10] | 92.7 | - | - | 116.4 | - | - | 89.1 | - | - | 119.2 | - | - |
| (eq.) B3LYP/6-31G**[10] | 89.8 | - | - | 118.1 | - | - | 89.1 | - | - | 117.1 | - | - |
| AM1[9] | 95.1 | - | - | - | - | - | 89.7 | 84.9 | - | - | - | 6.2 |
| PM3[9] | 94.5 | - | - | - | - | - | 88.8 | 87.6 | - | - | - | 4.5 |

*Table 6*

Bond angles of the cycles and the dihedral improper angle for the β-lactamic cycle of the conformers resulted from AM1 calculations for the (3S,5R,6R)-6-acetilamidopenicilanic acid with S pseudochirality at the N14 nitrogen atom, arranged according to the decreasing variation of the heat of formation, compared to some experimental and computed data in literature

| **Enegetic order** | **Angle (°)** | | | | | | | | | | | **Dihedral (°)** |
|---|---|---|---|---|---|---|---|---|---|---|---|---|
| | **C2-S1-C5** | **S1-C2-C3** | **C2-C3-N4** | **C3-N4-C5** | **S1-C5-N4** | **C5-N4-C7** | **N4-C5-C6** | **C5-C6-C7** | **C6-C7-N4** | **S1-C5-C6** | **C3-N4-C7** | **N4-C5-C6-C7** |
| 5am1 | 95.125 | 107.351 | 111.721 | 114.884 | 110.107 | 93.857 | 89.256 | 85.206 | 91.338 | 121.785 | 122.903 | 4.220 |
| 6am1 | 95.112 | 107.363 | 111.709 | 114.937 | 110.123 | 93.824 | 89.288 | 85.193 | 91.372 | 121.813 | 122.799 | 4.092 |
| 7am1 | 94.514 | 107.265 | 111.313 | 115.001 | 109.436 | 93.746 | 89.059 | 84.960 | 91.466 | 121.355 | 123.534 | 6.298 |
| 8am1 | 94.501 | 107.261 | 111.295 | 115.034 | 109.456 | 93.715 | 89.085 | 84.953 | 91.497 | 121.351 | 123.455 | 6.222 |

## CONCLUSIONS

The AM1 method gives only 8 distinct conformers of the (3S,5R,6R)-6-acetylamidopenicillanic acid and the energy difference between the lowest and highest energy conformers is of 7.12 kcal/mol. A good concordance between the geometry of the AM1 minimum energy conformer and the experimental geometry was obtained. There are no major differences between the results obtained with the AM1 semiempirical MO method and the ab initio and ab intio/DFT methods. The AM1 method gives three distinctive classes of bending of the thiazolidinic and β-lactamic rings and three classes of puckered thiazolidinic rings. The substituents at the C6 carbon atom influence significantly the number of conformers of the (3S,5R,6R)-6-acetylamidopenicillanic acid and the molecular and electronic structure of these conformers.

## REFERENCES


1. C. D. Nenițescu, *"Chimie organică"* Ed. 6-a, Vol. 2, Editura Didactică şi Pedagogică, Bucureşti, 1968, p. 629-630
2. G. P. Moss, *Basic Terminology of Stereochemistry (IUPAC Recommendations 1996)*: http://www.chem.qmul.ac.uk/iupac/stereo/
3. E. H. Flynn, (Ed.), *"Cephalosporins and Penicillins. Chemistry and Biology"*, Academic Press, New York, London, 1972,
4. G. I. Georg, (Ed.), *"The Organic Chemistry of β-Lactams"*, Academic Press, New York, 1993,
5. D. J. Tipper, J. L. Strominger, *Mechanism of Action of Penicillins: A Proposal Based on their Structural Similarity to Acyl-D-Alanyl-D-Alanine, Proc. Natl. Acad. Sci. U. S. A.*, **1965,** *54*, 1133-1141,
6. K. Izaki, M. Matsuhashi, J. L. Strominger, *Glycopeptide Transpeptidase and D-Alanine Carboxypeptidase: Penicillin-Sensitive Enzymatic Reactions*, *Proc. Natl. Acad. Sci. U. S. A.*, **1966,** *55*, 656-663,
7. N. Georgopapadakou, S. Hammaström, J. L. Strominger, *Isolation of the Penicillin-Binding peoptide from D-Alanine Carboxypeptidase of Bacillus Subtilis*, *Proc. Natl. Acad. Sci. U. S. A.*, **1977,** *74*, 1009-1012,
8. D. D. Boyd, *β-Lactam Antibacterial Agents: Computational Chemistry Investigations,* in A. Greenberg, C. M. Breneman, J. F. Liebman, (Eds.), *"The Amide Linkaje: Selected Structural Aspects in Chemistry, Biochemistry, and Materials Science",* John Wiley & Sons, Inc., New York, London, **2000**, Chap. 11,
9. J. Frau, J. Donoso, F. Muñoz, F. García Blanco, *Semiempirical calculations of the hydrolysis of penicillin G, J. Mol. Struct. (Theochem),* **1997,** *390,* 255-263,
10. A. Peña-Gallego, E. M. Cabalerio-Lago, A. Fernádez-Ramos, J. M. Hermida-Ramón, E. Martinez-Núñez, *An ab initio study of a model compound of penicillins, J. Mol. Struct. (Theochem),* **1999,** *491,* 177-185,
11. Frau J. Coll M. Vilanova B. Llinas A. Donoso J. Muñoz F., *Ab initio study of the chemical reactivity of oxo-beta-lactam structure*, *Internet J. Chem.,* **1999** *2*(16):NIL_3-NIL_12,
12. A. Nangia, G. R. Desiraju, *Axial and equatorial conformations of penicillins, their sulphoxides and sulphones: the role of N-H···S and C-H···O hydrogen bonds, J. Mol. Struct.,* **1999,** *474,* 65-79.
13. N. Diaz, D. Suárez, T. L. Sordo, *Theoretical Study of the Water-Assisted Aminolysis of β-Lactams. Implications for the Reactionbetween Human Serum Albumin and Penicillins, J. Am. Chem. Soc.,* **2000,** *122*, 6710-6719,
14. E. Gálvez-Ruano, I. Iriepa, A. Morreale, D. B. Boyd, *Superposition-based protocol as a tool for determining bioactive conformers. I. Application to ligands of the glyceric receptor (GlyR), J. Mol. Graphics Modell.,* **2001,** *19*, 331-337; 391-385,
15. N. Diaz, D. Suárez, T. L. Sordo, *Conformational Properties of Penicillins: Quantum Chemical Calculations and Molecular Dynamics Simulations of Benzylpenicillin, J. Comput. Chem.,* **2003,** *24*, 1864-1873,
16. Ira N. Levine, *"Quantum Chemistry",* 5th Edition, Prentice Hall, Inc., Upper Saddle River, New Jersy 07458, **2000,** Chap. 15, Chap. 17
17. *** ChemPlus 1.6™, *„Extension for HyperChem®, Molecular Modeling for Windows™",*Hypercube, Inc., Gainesville, Florida, USA, 1994, Chap. 8.
18. A. E. Howard, P. K. Kolman, *An Analysis of Current Methodologies for Conformational Searching of Complex Molecules, J. Med. Chem.,* **1988,** *31,* 1669-1674.
19. C. J. Cramer, *"Essentials of Computational Chemistry. Theory and Methods", Second Ed.,* John Wiley & Sons, Ltd., Chichester, 2004, p. 151.
20. http://www.middlebury.edu/~ch0337/atteridge/penicillin/fig1.gif
21. Y. Won. *Crystal Geometry optimization of β-Lactam Antibiotics Using MMFF Parameters, Bull. Korean Chem. Soc.,* **1995,** *16,* 944-952.